Identification of different putative outer membrane electron conduits necessary for Fe(III) citrate, Fe(III) oxide, Mn(IV) oxide, or electrode reduction by *Geobacter sulfurreducens*

Fernanda Jiménez Otero[a,b], Chi Ho Chan[a], Daniel R. Bond[a,b,c]

BioTechnology Institute[a], Department of Biochemistry, Molecular Biology, and Biophysics[b], Department of Plant and Microbial Biology[c] University of Minnesota-Twin Cities, Saint Paul MN 55108

Running title: Novel putative electron conduits of *G. sulfurreducens*

Send all correspondence to:

Daniel R. Bond

140 Gortner Laboratory

1479 Gortner Ave

St. Paul, MN 55108

dbond@umn.edu

Keywords: *Geobacter*, extracellular electron transfer, multiheme cytochrome, *c*-type cytochrome conduit

ABSTRACT

At least five gene clusters in the *Geobacter sulfurreducens* genome encode putative 'electron conduits' implicated in electron transfer across the outer membrane, each containing a periplasmic multiheme *c*-type cytochrome, integral outer membrane anchor, and outer membrane redox lipoprotein(s). Markerless single gene cluster deletions and all possible multiple deletion combinations were constructed and grown with soluble Fe(III) citrate, Fe(III)- and Mn(IV)-oxides, and graphite electrodes poised at +0.24 V and -0.1 V vs. SHE. Different gene clusters were necessary for reduction of each electron acceptor. During metal oxide reduction, deletion of the previously described *omcBC* cluster caused defects, but deletion of additional components in an Δ*omcBC* background, such as *extEFG,* were needed to produce defects greater than 50% compared to wild type. Deletion of all five gene clusters abolished all metal reduction. During electrode reduction, only the Δ*extABCD* mutant had a severe growth defect at both redox potentials, while this mutation did not affect Fe(III)-oxide, Mn(IV)-oxide, or Fe(III) citrate reduction. Some mutants containing only one cluster were able to reduce particular terminal electron acceptors better than wild type, suggesting routes for improvement by targeting specific electron transfer pathways. Transcriptomic comparisons between fumarate and electrode-based growth showed all of these *ext* clusters to be constitutive, and transcriptional analysis of the triple-deletion strain containing only *extABCD* detected no significant changes in expression of known redox proteins or pili components. These genetic experiments reveal new outer membrane conduit complexes necessary for growth of *G. sulfurreducens*, depending on the available extracellular electron acceptor.

IMPORTANCE

Gram-negative metal-reducing bacteria utilize electron conduits, chains of redox proteins spanning the outer membrane, to transfer electrons to the extracellular surface. Only one pathway for electron transfer across the outer membrane of *Geobacter sulfurreducens* has been linked to Fe(III) reduction. However, *G. sulfurreducens* is able to respire a wide array of extracellular substrates. Here, we present the first combinatorial genetic analysis of five different electron conduits via creation of new markerless deletion strains and complementation vectors. Multiple conduit gene clusters appear to have overlapping roles, including two that have never been linked to metal reduction. Another recently described cluster (ExtABCD) was the only electron conduit essential during electrode reduction, a substrate of special importance to biotechnological applications of this organism.

INTRODUCTION

Microorganisms capable of extracellular respiration can alter the redox state of particulate metal oxides in soils and sediments, controlling their solubility and bioavailability (1–6). To respire with extracellular metals, bacteria must first transfer electrons from the cell interior to outer surface redox proteins, requiring unique transmembrane pathways compared to growth with intracellularly-reduced compounds. The use of surface-exposed electron transfer proteins and conductive appendages by these organisms presents opportunities for transformation of heavy metals, biological nanoparticle synthesis, and a new generation of microbially-powered electrochemical devices using bacteria grown on electrodes (7–13).

An extracellular electron transfer strategy must overcome several challenges. In Gram-negative cells, a conductive pathway capable of crossing the inner membrane, periplasm, and outer membrane must first be constructed (14, 15). Such pathways are capable of delivering electrons to soluble metals or redox-active molecules, but insoluble metal oxides present additional barriers. Fe(III)- and Mn(IV)-oxides vary widely in chemistry, surface charge, redox state, and surface area, thus an additional suite of proteins or appendages such as pili may be needed to link cell surfaces with different terminal minerals (16–18).

Many metal-reducing bacteria can also transfer electrons to electrodes (8, 19–21). Unlike metal oxide particles, electrodes represent an unlimited electron acceptor allowing cells in contact with the inorganic surface to support growth of more distant

cells, if they can create a conductive network of proteins that relay electrons to cells at the electrode. The physiological and chemical differences between soluble metals, metal particles, and electrodes raises the possibility that different electron transfer proteins may be needed to access each kind of extracellular mineral, surface, or molecule.

A model organism widely studied for its ability to reduce a diversity of metals and electrodes is the δ-Proteobacterium *Geobacter sulfurreducens*, and recent work supports a model where different electron transfer proteins are used depending on substrate conditions. At the inner membrane where electrons first leave the quinone pool, a combination *c*- and *b*-type cytochrome CbcL (22) is only required when extracellular metals and electrodes are below redox potentials of -0.1 V vs. SHE, while the inner membrane *c*-type cytochrome ImcH (23), becomes essential if acceptors are at higher redox potentials (18). In another example, in the extracellular matrix beyond the cell surface, chemistry rather than redox potential appears to delineate which proteins are essential for electron transfer. The secreted cytochrome OmcZ and pili-based appendages are primarily linked to electrode growth, while the secreted cytochrome PgcA enhances reduction of Fe(III)-oxides without affecting electrode growth (24–31). Between the initial CbcL/ImcH-dependent event of inner membrane proton motive force generation and extracellular pili/OmcZ/PgcA interactions lies the outer membrane, a less understood barrier that was recently found to contain electron transfer proteins of surprising complexity (32–34).

The only known mechanism for non-diffusive electron transfer across the outer membrane is through a transmembrane 'electron conduit', consisting of an integral outer membrane protein anchoring a periplasmic multiheme cytochrome to an outer surface lipoprotein cytochrome. By linking redox active cofactors within a membrane-spanning complex, electron flow is permitted (32, 35). The first electron conduit described was the ~210 kDa MtrCAB complex from *S. oneidensis*, which will catalyze electron transfer across membranes when purified and placed in lipid vesicles (36–38). The *mtrCAB* gene cluster is essential for reduction of all tested soluble metals, electron shuttles, metal oxides, and electrodes by *S. oneidensis* (37, 39, 40). Related complexes capped with an extracellular DMSO reductase allow *Shewanella* to reduce DMSO on the cell exterior, while similar outer membrane conduits support inward electron flow by Fe(II)-oxidizing *Rhodopseudomonas* TIE-1 cells (41, 42).

In *G. sulfurreducens*, a gene cluster encoding the periplasmic cytochrome OmbB, the outer membrane integral protein OmaB, and lipoprotein cytochrome OmcB forms a conduit complex functionally similar to MtrCAB, though the two complexes lack any sequence similarity (34). This '*ombB-omaB-omcB'* gene cluster is duplicated immediately downstream in the *G. sulfurreducens* genome as the near-identical '*ombC-omaC-omcC'*, together forming the '*omcBC*' cluster. Antibiotic cassette insertions replacing *omcB,* as well as insertions replacing the entire '*ombB-omaB-omcB'* conduit, decrease growth with Fe(III) as an electron acceptor, but the impact differs between reports and growth conditions (43–45). This variability and residual electron transfer

activity suggested the presence of alternative pathways able to catalyze electron transfer across the outer membrane (33).

New evidence for undiscovered outer membrane complexes was recently detected in genome-wide transposon data, where insertions in *omcB* or *omcC* had no effect on *G. sulfurreducens* growth with electrodes poised at -0.1 vs. SHE, a low potential chosen to mimic the redox potential of Fe(III)-oxides (46). Transposon insertions within an unstudied four-gene cluster containing *c*-type cytochrome conduit signatures caused significant defects during growth on the same -0.1 V electrodes (46). Deletion of this new cluster, named *extABCD*, severely affected growth on low-potential electrodes, while Δ*extABCD* mutants still grew similar to wild type with Fe(III)-oxides. In contrast, deletion of the entire *omcBC* cluster had little impact on low-potential electrode growth (46). These data suggested that the outer membrane proteins essential for electron transfer across the membrane might vary depending on environmental conditions. However, these data involved only single deletions without complementation and did not test if different gene clusters were necessary across the full range of environmentally relevant conditions such as higher redox potentials, during growth with mineral forms such as Mn(VI), or when metals become soluble.

Using new markerless deletion methods, this study constructed mutants containing all combinations of the four putative conduit clusters on the genome of *G. sulfurreducens.* Each of these 15 mutants plus three strains containing expression vectors were then directly compared with five electron acceptors; Fe(III)- and Mn(IV)-oxides, poised

electrodes at two different redox potentials, and soluble Fe(III)-citrate. We found that during metal reduction the largest defects were in Δ*omcBC* strains, but deletion of the newly identified cluster *extEFG* in the Δ*omcBC* background was necessary to most severely inhibit Fe(III)-reduction, and deletion of all clusters was required to eliminate reduction of both soluble and insoluble metals. Strains containing only a single cluster showed preferences for reduction of different metals, such as the *extEFG*- and *extHIJKL*-only strains performing better with Mn(IV)-oxides than Fe(III)-oxides. When electrodes were the electron acceptor, only strains lacking *extABCD* showed a growth defect, and this effect was similar at all redox potentials. A strain still containing *extABCD* but lacking all other conduit clusters grew faster and to a higher final density on electrodes, and a complemented strain lacking all other conduit clusters expressing *extABCD* from a vector also grew faster than wild type. These data provide evidence that different *G. sulfurreducens* conduit clusters are necessary during extracellular electron transfer depending on the extracellular substrate.

(This article was submitted to an online preprint archive (47))

RESULTS

Description of putative outer membrane electron conduit gene clusters. At least five loci can be identified in the *G. sulfurreducens* genome encoding putative *c*-type cytochrome electron conduits. This identification is based on three key elements; (1) a

multiheme periplasmic *c*-type cytochrome, (2) an outer membrane integral protein with transmembrane ß-sheets, and (3) one or more outer membrane lipoproteins with redox cofactors (Fig. 1A). Two of these regions correspond to the well-studied OmcB-based (*omb*B-*oma*B-*omc*B, GSU2739-2737) conduit and its near-identical duplicate OmcC-based operon immediately downstream preceded by a TetR-family repressor partially truncated in its DNA-binding domain (*orfS*-*omb*C-*oma*C-o*mc*C, GSU2733-2731). For clarity, and due to the fact that *omaBC* and *ombBC* are identical, this region is referred to as the "*omcBC*" cluster. The well-characterized duplicate *omcBC* cluster was deleted as a single unit (see also Materials and Methods for additional information about the tendency of identical genes within this region to recombine during mutant construction and efforts taken to verify proper removal and reconstruction of *omcBC* genes).

The *ext* genes comprise three new clusters, named for their putative roles in extracellular electron transfer (46). Relative protein orientations were predicted using a combination of protein localization prediction software (48), integral membrane prediction software (49), and lipid attachment site prediction software (50). The *extABCD* (GSU2645-2642) cluster encodes ExtA, a periplasmic dodecaheme *c*-type cytochrome, ExtB, an outer membrane integral protein with 18 trans-membrane domains, and ExtCD, two outer membrane lipoprotein *c*-type cytochromes with 5 and 12 heme binding sites, respectively. The second cluster, *extEFG* (GSU2726-2724), encodes ExtE, an outer membrane integral protein with 21 trans-membrane domains, ExtF, an outer membrane lipoprotein pentaheme *c*-type cytochrome, and ExtG, a periplasmic dodecaheme *c*-type cytochrome. Kanamycin insertions in ExtG have been

197 shown to affect Fe(III)-oxide reduction, which in some annotations is referred to as
198 OmcV (51) despite its predicted periplasmic localization. For consistency with the
199 surrounding operon and to distinguish it from outer membrane cytochromes, the name
200 ExtG will be used in this work. The final cluster, *extHIJKL* (GSU2940-2936) lacks an
201 outer membrane *c*-type cytochrome, but encodes ExtH, a rhodanese-family lipoprotein,
202 ExtI, a 21 trans-membrane domain outer membrane integral protein, ExtJ, a small
203 periplasmic protein, and ExtKL, a periplasmic pentaheme *c*-type cytochrome followed
204 by a small hypothetical protein. A TGA stop codon encoding a predicted rare
205 selenocystine amino acid separates ExtK and ExtL, thus they may encode a single
206 protein (52).
207
208 A significant difference between *G. sulfurreducens* Ext clusters and the *S. oneidensis*
209 Mtr conduits (35), is that the *mtr* clusters in *S. oneidensis* are paralogs. The periplasmic
210 MtrA and MtrD cytochromes share over 50% identity, are similar in size and heme
211 content, and can cross-complement (53). The lipoprotein outer surface cytochromes of
212 *Shewanella* also demonstrate high sequence, functional, and structural conservation
213 (32, 53–55). In contrast, no component of the Ext or OmcB complexes share any
214 homology. For example, the predicted periplasmic *c*-type cytochromes ExtA, ExtG,
215 ExtK, and OmaB vary in size from 25 to 72 kDa, contain 5 to 15 hemes, and share 18%-
216 26% identity (Fig. 1B).
217
218 To screen for physiological roles of these loci, single cluster mutants were first
219 constructed in an isogenic background, comprising Δ*extABCD,* Δ*extEFG,* Δ*extHIJKL,*

and Δ*omb*B-*oma*B-*omc*B-*orfS*-*omb*C-*oma*C-o*mc*C (abbreviated as Δ*omcBC*) mutants. Previous studies have reported complementary roles of OmcB and OmcC (43, 45), thus the entire *omcBC* cluster was removed to screen for conditions under which this pair of homologous conduits were necessary. As these single mutant strains lacked any antibiotic cassettes, they could be used as backgrounds for further double and triple deletions. Multiple cluster deletion mutants leaving only one conduit cluster on the genome are referred to by their remaining cluster, e.g. "*extABCD*$^{+}$" contains only *extABCD* and is constructed by Δ*extEFG* Δ*extHIJKL* Δ*omcB*C, while the mutant lacking all *extABCD, extEFG, extHIJKL*, *omcB*-based and *omcC*-based clusters is referred to as "Δ5". After whole-genome resequencing of all terminal strains containing single clusters and the strain missing all clusters (such as *extABCD*$^{+}$ and Δ5) to verify no off-target mutations accumulated during the many rounds of insertion and recombination, all of these strains were tested under six different extracellular growth conditions varying in solubility, chemical composition, and redox potential.

Cells lacking single gene clusters have only partial reduction defects with Fe(III) citrate. Soluble Fe(III) citrate was the simplest extracellular electron acceptor tested in this study, requiring no attachment to a surface, and requiring no appendages such as a pili or secreted cytochromes for reduction. Under these conditions, no single cluster deletion eliminated the majority of soluble Fe(III) citrate reduction. The most severe defect was observed in the Δ*omcBC* cluster mutant, which grew slower than any other single mutant and reduced only 60% of Fe(III) citrate compared to wild type (Fig. 2A). Minor defects were also observed for Δ*extEFG* and Δ*extHIJKL*, while Δ*extABCD*

reduced Fe(III) citrate at wild-type levels. These results suggested that more than one cluster was necessary for wild type soluble Fe(III) reduction.

Any one gene cluster is sufficient for partial Fe(III) citrate reduction, and deletion of all 5 clusters eliminates electron transfer to this substrate. Deletion of the full suite of clusters was the only combination that eliminated all residual electron transfer to Fe(III) citrate (Fig. 2B). When multiple-deletion strains still containing one cluster were tested for Fe(III) citrate reduction, results supported key roles for *omcBC* and *extABCD* in soluble metal reduction, and little involvement by *extEFG* or *extHIJKL*. For example, Fe(III) citrate reduction by *omcBC*$^{+}$ and *extABCD*$^{+}$ was comparable to that of wild type, while *extEFG*$^{+}$ and *extHIJKL*$^{+}$ strains reduced Fe(III) citrate to just 20% of wild type.

Only strains lacking both *omcBC* and *extABCD* had a significant defect in Fe(III) citrate reduction. Because Δ*omcBC* demonstrated the largest defect in Fe(III) citrate reduction, additional deletions in this background were tested for their ability to reduce this substrate (Fig. 2C). Only the double cluster deletion mutant Δ*omcBC* Δ*extABCD* reduced Fe(III) citrate at a significantly lower rate compared to the Δ*omcBC* strain, which agreed with the robust growth seen in strains containing only *omcBC*$^{+}$ or *extABCD*$^{+}$. The Δ*omcBC* Δ*extABCD* mutant (still containing both *extEFG* and *extHIJKL*) reduced Fe(III) citrate poorly, to the same level as their single-cluster strains containing only *extEFG*$^{+}$ or *extHIJKL*$^{+}$ (Fig. 1B vs. Fig. 2C). These data suggested that when both *extEFG* and *extHIJKL* remained in the genome, their contribution was not additive.

Not shown in Fig 2 is metal reduction data for intermediate deletion mutants with no additional phenotype such as Δ*extEFG* Δ*extHIJKL*. Experiments performed after such double mutants were constructed revealed no changes that deviated from wild type or their parent single-cluster deletions. Only intermediate strains with additive phenotypes, such as strains in the Δ*omcBC* background, are shown in Fig 2.

Expression of single conduit clusters from vectors is sufficient to recover Fe(III) citrate reduction. When compared to empty-vector controls, complementation of the Δ5 strain with single *omcB (*as *ombB-omaB-omcB*) or *extABCD* clusters restored Fe(III) citrate reduction to levels within 90% of the respective *omcBC*$^{+}$ and *extABCD*$^{+}$ strains (Fig. 2D). Previous studies have also shown that expression of only the *omcB*-based cluster is sufficient to rescue ferric citrate reduction defects in a Δ*omcBC* strain (45), but *extABCD* has never been used to rescue a respiratory phenotype. These data are the first evidence that a putative outer membrane complex other than those encoded in *omcB* could be sufficient for extracellular metal reduction in *Geobacter*.

Only strains lacking multiple gene clusters have significant defects in Fe(III)- and Mn(IV)-oxide reduction. Particulate metal oxides represent substrates of additional complexity, requiring pili and additional cytochromes for long-range electron transfer to particles or surfaces after transmembrane electron transfer. Because they are not hypothesized to act as the interface with distant electron acceptors, it was possible the outer membrane complex mutants would show less specificity during reduction of Fe(III) or Mn(IV) oxides. However, trends remained similar to Fe(III) citrate, where deletion of

289 single conduit clusters in *G. sulfurreducens* only had modest effects on metal oxide
290 reduction (Fig. 3A and C) and additional conduit cluster deletions were needed to
291 severely impact growth (Fig. 3B and D). The most severe defect was again observed in
292 the Δ*omcBC* cluster mutant, which reduced 68% of Fe(III)-oxide compared to wild type
293 (Fig. 3A). Minor defects were observed for single Δ*extEFG* and Δ*extHIJKL* deletions,
294 while Δ*extABCD* reduced Fe(III)-oxide near wild-type levels. In contrast, none of the
295 single mutants displayed defects with Mn(IV)-oxides (Fig. 3C).
296
297 Unlike soluble metal reduction, however, results supported roles for *omcBC* and *extEFG*
298 in metal oxide reduction and little involvement by *extABCD*. For example, in strains
299 containing only one cluster, Fe(III)-oxide reduction by *omcBC*$^{+}$ was nearly 80% of wild
300 type, *extEFG*$^{+}$ was over 60%, but the *extABCD*$^{+}$ strain reduced less than 30% of wild
301 type. Similarly, the *omcBC*$^{+}$, *extEFG*$^{+}$, and *extHIJKL*$^{+}$ strains achieved about 80% of
302 wild type Mn(IV)-reduction at 80 hours, but the *extABCD*$^{+}$ strain again displayed poor
303 Mn(IV)-oxide reduction. As with soluble metal reduction, deletion of the full suite of
304 clusters was necessary to eliminate all residual electron transfer to either Fe(III)- or
305 Mn(IV)-oxides (Fig. 3B and D).
306
307 **Only strains lacking both *omcBC* and *extEFG* had a significant defect in Fe(III)-**
308 **and Mn(IV)-oxide reduction.** Since Δ*omcBC* demonstrated the largest defect in Fe(III)-
309 oxide reduction, additional deletions in this background were tested during Fe(III) and
310 Mn(IV)-oxide reduction (Fig. 4). Fe(III)-oxide reduction by Δ*omcBC* Δ*extEFG* was less
311 than 25% of wild type, while the Δ*omcBC* Δ*extABCD*, and Δ*omcBC* Δ*extHIJKL* strains

312 still reduced Fe(III)-oxides similar to the Δ*omcBC* strain. The additive effect from
313 Δ*extEFG* agreed with data from mutants containing single clusters, where *omcBC*$^{+}$,
314 and *extEFG*$^{+}$ showed the best reduction. The Δ*omcBC* Δ*extEFG* strain also had a
315 severe Mn(IV)-oxide reduction defect. However, unlike Fe(III)-oxide reduction, the
316 Δ*omcBC* Δ*extABCD* and Δ*omcBC* Δ*extHIJKL* double deletion strains had only a modest
317 Mn(IV) reduction defect, suggesting higher contributions of *extABCD* and *extHIJKL*
318 clusters during Mn(IV) compared to Fe(III) reduction.
319
320 The poor growth of the Δ*omcBC* Δ*extEFG* mutant with insoluble metals was surprising,
321 since this strain still contained *extHIJKL*. When e*xtHIJKL* was the only cluster
322 remaining, the *extHIJKL*$^{+}$ strain reduced up to 50% of Fe(III)-oxide and 75% of Mn(IV)-
323 oxide compared to wild type (Fig. 3B and D; Table 2). This was a rare case where
324 performance of a mutant containing the single cluster performed better than predicted
325 by single and double mutants, and raises the hypothesis that *extHIJKL* expression or
326 function is partially inhibited by the presence of *extABCD*. No other *ext* or *omc* cluster
327 showed this kind of behavior with soluble or insoluble metals.
328
329 **Expression of single conduit clusters partially recovers Fe(III)- and Mn(IV)-oxide**
330 **reduction.** Plasmids containing constiutive *ombB-omaB-omcB* or *extABCD* clusters
331 resulted in partial recovery (Fig. 5), consistent with the intermediate phenotypes
332 displayed by mutants retaining these single clusters on the genome. Expression of the
333 *omcB* cluster reestablished Fe(III)-oxide reduction to a level less than that seen in the
334 *omcBC*$^{+}$ strain containing the full duplicated cluster in its original context, suggesting

that both *omcB* and *omcC* are necessary (Fig. 4B). Expressing *extABCD* from a plasmid restored Fe(III)-oxide reduction in the Δ5 strain near the low levels of the *extABCD*$^+$ strain, and reduction of Mn(IV)-oxides by *omcB* or *extABCD*-expressing strains was even lower. These data again agreed with the partial reduction phenotype of mutant strains containing only *extABCD*.

Mutants lacking *extABCD* are defective in electrode growth at all redox potentials, while mutants containing only *extABCD* outperform wild type. In contrast to metal reduction, when strains were grown as biofilms on electrodes poised at high (0.24 V vs. SHE) or low (-0.1 V, (46)) redox potentials, only Δ*extABCD* mutants showed a defect in both the rate and extent of growth. Mutants lacking the *omcBC* and *extEFG* clusters grew at similar rates as wild type, while Δ*extHIJKL* demonstrated a lag before growing with a similar doubling time as wild type (Fig. 6A). In all experiments, Δ*extABCD* grew poorly, without a clear exponential phase. The apparent doubling time of Δ*extABCD* was longer than 20 h, or over 3-fold slower than wild type, and only reached 20% of wild type final current density, or 116 ± 33 μA/cm^2 vs. 557 ± 44 μA/cm^2 (n ≥ 5 per strain).

Mutants containing only one gene cluster (*extABCD*$^+$, *extEFG*$^+$, *extHIJKL*$^+$, *omcBC*$^+$) as well as a mutant lacking all gene clusters (Δ5) were then analyzed for growth on electrodes. The Δ5 mutant grew at the same low, nonexponential rate as the Δ*extABCD* single mutant at both redox potentials, suggesting that none of the additional clusters were responsible for residual growth rate originally seen in Δ*extABCD*. In contrast, *extABCD*$^+$ grew faster than wild type (4.5 ± 0.2 h vs. 6.5 ± 0.3 h doubling time, n ≥ 9)

and reached a final current density 40% higher than wild type (768 ± 52 μA/cm^2 vs. 557 ± 44μA/cm^2, n≥9). All other multiple-deletion strains containing only one cluster grew as poorly as the Δ5 mutant, further indicating that under these conditions, *extEFG*, *extHIJKL,* and *omcBC* were not necessary or sufficient to restore electron transfer to electrodes (Fig. 6B). We were unable to identify the origin of the slow growth enabling residual electron transfer to electrodes, although *G. sulfurreducens* contains at least 3 other multiheme cytochrome-rich regions with conduit-like signatures that remain to be examined.

A 5-conduit deletion mutant expressing *extABCD* has a faster growth rate on electrodes than wild type. To further investigate the specific effect of *extABCD* on electrode growth, *extABCD* was provided on a vector in the Δ5 strain. The 3-gene *omcB* conduit cluster (*omb*B-*oma*B-*omc*B) was also placed in the Δ5 strain using the same vector, and both were compared to wild type cells containing the empty vector. While the plasmid is stable for multiple generations, routine vector maintenance requires growth with kanamycin, and kanamycin carry-over into biofilm electrode experiments is reported to have deleterious effects on electrode growth (23, 56). Thus, we first re-examined growth of the empty vector strain. When selective levels of kanamycin (200 μg·ml^{-1}) were present in electrode reactors, colonization slowed and final current production decreased 74% even though cells carried a kanamycin resistance cassette. At levels resulting from carry-over during passage of cells into the electrode reactor (5 μg·ml^{-1}) growth rate of vector-containing cells was not affected, but final current was decreased up to 30%, suggesting interference with biofilm formation rather than

respiration (Fig. 7A). All subsequent complementation was performed in the presence of 5 $\mu g \cdot ml^{-1}$ residual kanamycin and compared to these controls.

Expressing the *omcB* conduit cluster in the Δ5 strain failed to increase growth with electrodes as electron acceptors. These data were consistent with the lack of an effect seen in Δ*omcBC* deletions, and the poor growth of *omcBC*$^{+}$ mutants that still contained both the OmcB and OmcC clusters in their native genomic context (Fig. 7B). In contrast, when *extABCD* was expressed on the same vector in the Δ5 background, colonization was faster and cells reached a higher final current density compared to wild type carrying the empty vector (421 ± 89 $\mu A/cm^2$ vs. 297 ± 11 $\mu A/cm^2$, n=3) (Fig. 7B). This enhancement by plasmid-expressed *extABCD* (141% of wild type with empty vector) was similar to the positive effect observed in the *extABCD*$^{+}$ strain (137% of wild type) (Fig. 6B), and further supported the hypothesis that *extABCD* is both necessary and sufficient during growth with electrodes.

Growth of any two-conduit deletion mutant was unchanged from single-cluster strains (Fig. S1). For example, just as the mutant lacking *extABCD* produced the same phenotype as the Δ5 strain (Fig. 6), deletion of a second cluster from the Δ*extABCD* strain produced similar results as Δ*extABCD* alone, and no two-cluster combination of *omcBC*, *extEFG* or *extHIJKL* showed defects to suggest they were required during electrode growth conditions, or to indicate their presence affected expression of *extABCD*. The Δ*extABCD* and Δ5 strains were also monitored during extended

403 incubation times to determine if final current density increased after a prolonged
404 incubation period, but current remained unchanged even after 200 h (Fig. S2).
405
406 **Transcriptomic analysis reveals no differential expression of putative conduit**
407 **clusters during growth on electrodes, or off-target expression effects in**
408 ***extABCD*$^{+}$.** The importance of the *extABCD* gene cluster during electrode growth was
409 first discovered via genetic experiments (46), but none of the *ext* genes described here
410 were highlighted or examined in earlier studies measuring transcriptional or proteomic
411 changes. Data is available from microarray studies comparing stationary phase
412 electrode biofilms with >4 day old fumarate biofilms grown under electron donor
413 limitation (24), or comparing stationary phase electrode biofilms with Fe(III) citrate
414 grown cells (57). As mature biofilms contain many layers of inactive or slowly growing
415 cells (58), we conducted new experiments capturing both fumarate- and electrode-
416 grown cells during exponential growth to determine absolute levels of transcriptional
417 abundance for *ext* and *omc* genes, using RNAseq.
418
419 Figure 8A compares expression levels of wild type *G. sulfurreducens* during exponential
420 fumarate growth to exponential growth with electrodes, using data averaged from at
421 least 2 biological replicates under each condition. Despite the fact that this represents a
422 shift from planktonic cells using an intracellularly reduced acceptor to biofilms using an
423 extracellular acceptor, few genes undergo changes +/- $Log_2 > 2$. Highlighted in Fig 8A
424 are all annotated cytochromes and pili genes reported to be involved in metal or

electrode respiration, showing that nearly all of these were constitutively expressed between the two laboratory conditions of non-limiting electron acceptor.

Compared to the highly expressed *omcBC* genes, genes for *extABCD* and other *ext* clusters were expressed at levels equivalent to only 10-20% of *omcB* under both conditions, which may explain OmcB's dominance in prior gel-based heme stain identification and proteomic analyses. We did observe an overall trend of increased cytochrome and electron transfer gene expression during growth on electrodes, reflecting a general increase in extracellular respiratory processes, but these changes occurred in both essential and nonessential genes. Genes encoding the characterized inner membrane electron transfer proteins ImcH or CbcL also did not change significantly in expression between these two conditions, nor did any genes for periplasmic cytochromes or pili components known to be essential (18, 22, 23). As has been shown before (24), the well-characterized extracellular cytochrome *omcZ* was upregulated over 8-fold during electrode reduction, and a putative inner membrane *c*- and *b*-type cytochrome similar to CbcL that is up-regulated during Fe(III) reduction (*cbcBA)* also increased over 30-fold (51) (Fig. 8A). A table providing RPKM data for all genes studied in this paper, along with *omcZ* and *cbcBA*, is provided in Fig 8B. As none of the *extABCDEFGHIJKL* genes were strongly induced or repressed during electrode growth, and these genes were generally expressed at levels 1/10th of the *omcBC* locus, their absence from prior differential expression analyses is understandable.

A second question that often arises in the study of complex phenotypes is whether deletion of an important or highly expressed cluster such as *omcBC* affects expression of other genes, especially as phenotypes such as biofilm growth require secretion of complexes to the outer membrane, adhesion of cells to surfaces, and production of extracellular proteins such as pili (59–61). The fact that the *extABCD*$^{+}$ strain lacking 15 different genes always grew faster than wild type, and produced more current than wild type, raised a significant question regarding possible off-target effects on other aspects of metabolism. Therefore, the transcriptome of the *extABCD*$^{+}$ strain was analyzed under both fumarate- and electrode-respiring conditions, and compared to wild type.

No significant increase or decrease in expression of any previously studied electron transfer proteins were found during growth in fumarate, or during exponential growth on electrodes, when the *extABCD*$^{+}$ strain was compared to wild type (Fig. 8C-D). This further suggested the increased growth rate was not due to higher expression of an unknown gene enabling electron transfer or attachment. It also underscored the trend in *Geobacter* that many genes such as *omcB* are among the most highly expressed under laboratory conditions, yet these expression levels have not correlated with essentiality or function. The full data sets plotted on Figure 8 can be found in Table S2.

Summary of phenotypes for all Omc and Ext electron conduit gene cluster mutants. Table 2 summarizes all extracellular reduction phenotypes of single cluster deletions and deletions leaving only one conduit on the genome, adjusted to wild type performance. Each gene cluster was necessary under different conditions. Many of the

recently described *ext* gene clusters were necessary for wild-type metal reduction, yet few were sufficient. For example, *extEFG* and *extHIJKL* were necessary for Fe(III) citrate reduction, as strains lacking these clusters only reduced ~65% of wild type levels. But when only *extEFG* or only *extHIJKL* was present, they were not sufficient to reduce Fe(III) citrate at wild type levels. In contrast, the *omcBC* cluster or the *extABCD* cluster alone was necessary for Fe(III) citrate reduction, and the *extABCD* cluster alone was also sufficient for electrode growth. Deletion of all five conduit clusters resulted in complete elimination of metal reduction abilities, while some residual activity remained when the same Δ5 strain was grown using electrodes as terminal electron acceptor. These comparisons show each gene cluster is necessary under at least one of the conditions studied, and provides evidence for additional undiscovered mechanisms enabling transmembrane electron transfer during electrode growth.

DISCUSSION

Sequencing of the *G. sulfurreducens* genome revealed an unprecedented number of electron transfer proteins, with twice as many genes dedicated to respiratory and redox reactions as organisms with similarly-sized genomes (62). Out of 111 *c*-type cytochromes, 43 had no known homolog, and many were predicted to reside in the outer membrane. The large complement of outer membrane redox proteins in *G. sulfurreducens* became even more of an anomaly as the simpler electron transfer strategy of metal-reducing *S. oneidensis* emerged. If *Shewanella* only requires a single inner membrane cytochrome and a single outer membrane conduit to reduce a

493 multitude of substrates (36, 39, 40, 53), why does *Geobacter* have so many
494 cytochromes?
495
496 Evidence that more than one *G. sulfurreducens* outer membrane pathway exists for
497 reduction of extracellular substrates has accumulated in at least 11 separate studies
498 since discovery of OmcB (34, 43, 45). Deletion of *omcB* impacted Fe(III)-reduction, but
499 had little effect on U(IV) or Mn(IV)-oxide reduction (51, 63). A Δ*omcB* suppressor strain
500 evolved for improved Fe(III)-citrate growth still reduced Fe(III)-oxides poorly (44).
501 Strains lacking *omcB* grew similar to wild type on electrodes in four different studies,
502 (24, 29, 57, 64), and OmcB abundance was shown to be lowest on cells near electrodes
503 (65). An insertional mutant lacking six secreted or outer membrane-associated
504 cytochromes in addition to OmcB still demonstrated Fe(III)-oxide reduction (66). After
505 replacing the entire *omcBC* region with an antibiotic cassette and still finding residual
506 Fe(III)-reducing ability, Liu *et al.* (2015) speculated that other *c*-type cytochrome
507 conduit-like clusters in the genome might be active. Most recently, Tn-seq analysis of
508 electrode-grown cells found little effect of *omcB* cluster mutations, yet noted significant
509 defects from insertions in unstudied clusters with *c*-type cytochrome features (46). This
510 combined evidence led us to seek alternative conduit gene clusters that could address
511 both the longstanding mystery of growth by *omcB* mutants and the complexity of
512 electron transfer proteins in the *Geobacter* genome.
513
514 The genetic analysis presented here supports a role for these unstudied conduit gene
515 clusters during extracellular respiration. All mutants still containing at least one cluster

516 retained a partial ability to reduce metals, while deletion of the entire *omcBC* region,
517 plus all three *ext* clusters, finally was able to eliminate metal reduction. This need to
518 delete more than one cluster helps explain variability reported with other mutants, and
519 the rapid evolution of suppressors in Δ*omcB* mutants.
520
521 In the case of electrodes at both high and low potential, only deletion of *extABCD*
522 altered phenotypes. Additionally, a strain with only *extABCD* remaining on the genome
523 outperformed wild type in terms of growth rate and final current density when grown on
524 electrodes. Since expression of *extABCD* was also able to restore reduction of the
525 soluble acceptor Fe(III) citrate, this cluster can confer the phenotype of extracellular
526 respiration under a condition where pili and secreted cytochromes are not known to be
527 important. Overall, these data show that for all tested metal acceptors, more than one
528 conduit cluster is necessary for wild type levels of reduction, any one cluster can
529 support partial reduction of may metals, and only one cluster can be linked to electrode
530 respiration.
531
532 Genetic analyses are typically a first step, designed to reveal which genes are
533 necessary for a phenotype, and worthy of further study. Biochemical and biophysical
534 analyses will be needed to prove (1) if products of *ext* gene clusters indeed function as
535 conduits to transfer electrons across the outer membrane, and (2) identify the proteins
536 or metals these complexes interact with to explain why these clusters seem so tightly
537 linked to growth with certain substrates. Expression analyses failed to detect large
538 differences in *ext* or *omcBC* family genes during transitions between acceptors, arguing

539 against changes in expression as an explanation for specificity. Our ability to
540 complement growth with electrodes in the Δ5 mutant by expressing *extABCD* from a
541 vector, while the *omcB* conduit could not complement growth, further argues against
542 expression differences causing these phenotypes. Unknown post-transcriptional events
543 could be caused by the absence of different gene clusters, but the genetic conclusion
544 that these gene clusters are necessary remains the same.
545
546 To reduce metal particles or surfaces likely requires each membrane-bound complex to
547 interact with extracellular proteins such as OmcZ, OmcS, PgcA, or pili, to aid transfer of
548 electrons to the final destination. If these partner proteins are not expressed or made
549 available under all conditions, an outer membrane complex may not be capable of
550 contributing to respiration. In the case of soluble metals such as Fe(III) citrate, conduit
551 complexes should be able to directly reduce the acceptor, making apparent specificity
552 more likely due the ability of the complex(es) to interact with Fe(III) directly.
553
554 It is also important to consider lessons from insertional deletions in *G. sulfurreducens*,
555 such as the diheme peroxidase MacA. Initially hypothesized to be an inner membrane
556 quinone oxioreductase, based on the defective phenotype of Δ*macA* mutants during
557 Fe(III)-citrate reduction (67), this phenotype was later explained by Δ*macA* mutants not
558 expressing *omcB*, as the Δ*macA* phenotype could be rescued by expressing *omcB* from
559 a vector (68, 69). As MacA is now known to instead be a soluble peroxidase, oxidative
560 stress in early Δ*macA* studied could have resulted in global downregulation of
561 cytochromes. In our work, the availability of every combination of gene cluster deletion

and acceptor condition allows many general downregulation hypotheses to be eliminated. For example, if deletion of *extABCD* suppressed production of pili or cytochromes such as OmcS, all Δ*extABCD* mutants would be predicted to show both an electrode and metal oxide defect, which we did not observe.

Initial transcriptomic surveys also failed to find severe or off-target transcriptional effects on known electron transfer proteins from deletion of *omb*B-*oma*B-*omc*B-*orfS*-*omb*C-*oma*C-*omc*C, *extEFG*, or *extHIJKL*, that could explain the enhanced growth of *extABCD*$^{+}$. The fact that only the *omb*B-*oma*B-*omc*B cluster was necessary to restore Fe(III) citrate reduction further indicated that *orfS* was not essential. However, all of these deletions removed many parts of the genome which were not tested for complementation by single genes, leaving open the possibility of regulatory interactions. Also, in a complex system such as this, post-translational events such as polymerization of pilin monomers into filaments, extracellular cytochrome secretion could be affected by the absence of specific proteins under specific conditions. It is difficult to detect negative interactions via RNAseq or proteomic analyses when mutants fail to grow, but such effects should be addressed in future suppressor and heterologous expression studies, now that these clusters have been identified.

Insights from similar gene clusters in related organisms. It remains difficult to predict any function for multiheme cytochromes based on sequence alone, so their genetic context may reveal other clues to their role, and aid identification of such clusters in other genomes. None of the *ext* regions fits the pattern of the *mtr* 3-gene

585 'cytochrome conduit' operon of one small (~40 kDa) periplasmic cytochrome, an integral
586 outer membrane protein, and one large (>90 kDa) lipoprotein cytochrome. For example,
587 *extABCD* includes two small lipoprotein cytochromes, *extEFG* is part of a hydrogenase-
588 family transcriptional unit, and *extHIJKL* contains a rhodanese-like lipoprotein instead of
589 an extracellular cytochrome (Fig. 1).
590
591 Specifically, the transcriptional unit beginning with *extEFG* includes a homolog of YedY-
592 family periplasmic protein repair systems described in *E. coli* (70), followed by a NiFe
593 hydrogenase similar to bidirectional Hox hydrogenases used to recycle reducing
594 equivalents in Cyanobacteria (71–73). Rhodanase-like proteins related to ExtH typically
595 are involved in sulfur metabolism (74–76) and an outer surface ExtH/rhodanese-like
596 protein is linked to extracellular oxidation of metal sulfides by *Acidithiobacillus*
597 *ferrooxidans* (77). Deletion of *extI* in *G. sulfurreducens* causes a severe defect in
598 selenite and tellurite reduction (78). These links to metabolism of hydrogen, sulfur, and
599 other oxyanions suggest roles outside of metal reduction, and future genomic searches
600 for electron conduit clusters should consider the possibility of non-cytochrome
601 components, such as FeS clusters, as the exposed lipoprotein.
602
603 Now that genes from *ext* operons can be used in searches of other genomes, an
604 interesting pattern emerges in putative conduit regions throughout Desulfuromonadales
605 strains isolated from freshwater, saline, subsurface, and fuel cell environments (Fig. 9).
606 In about 1/3 of cases, an entire cluster is conserved intact, such as *extABCD* in *G.*
607 *anodireducens, G. soli,* and *G. pickeringii* (Fig. 9B). However, when differences exist,

608 they are typically non-orthologous replacements of the outer surface lipoprotein, such
609 as where *extABC* is followed by a new cytochrome in *G. metallireducens,*
610 *Geoalkalibacter ferrihydriticus,* and *Desulfuromonas soudanensis.* Conservation of the
611 periplasmic cytochrome with replacement of the outer surface redox lipoprotein also
612 occurs frequently in the *omcB* and *extHIJKL* clusters (Fig 9A and D). For example, of 18
613 *extHIJKL* regions, 10 contain a different extracellular rhodanese-like protein with
614 *extIJKL*, each with less than 40% identity to *extH*. This remarkable variability in
615 extracellular components, compared to conservation of periplasmic redox proteins,
616 suggests much higher rates of gene transfer and replacement of domains that are
617 exposed to electron acceptors and the external environment.
618
619 **Summary.** The data presented here significantly expands the number of genes
620 encoding outer membrane redox proteins necessary during electron transfer in *G.*
621 *sulfurreducens* and highlights a key difference in the *Geobacter* electron transfer
622 strategy compared to other model organisms. In general, the pattern of multiple genes
623 encoding seemingly overlapping or redundant roles is less like solitary respiratory
624 reductases, and more reminiscent of systems in cellulolytic bacteria that produce
625 numerous similar β-glucosidases to attack a constantly changing polysaccharide
626 substrate (36, 40, 79). A need for multiple outer membrane strategies could be a
627 response to the complexity of metal oxides during reduction; minerals rapidly diversify to
628 become multiphase assemblages of more crystalline phases, the cell:metal interface
629 can become enriched in Fe(II), and organic materials can bind to alter the surface (80–
630 82). Constitutively expressing an array of electron transfer pathways could make cells

631 competitive at all stages with all electron acceptors, allowing *Geobacter* to outgrow

632 more specialized organisms during rapid perturbations in the environment.

633

EXPERIMENTAL PROCEDURES

Growth conditions.

All experiments were performed with our laboratory strain of *Geobacter sulfurreducens* PCA as freshly streaked single colonies from freezer stocks. Anaerobic NB medium (0.38 g/L KCl, 0.2 g/L NH_4Cl, 0.069 g/L $NaH_2PO_4H_2O$, 0.04 g/L $CaCl_22H_2O$, 0.2 g/L $MgSO_47H_2O$, 1% v/v trace mineral mix, pH 6.8, buffered with 2 g/L $NaHCO_3$ and flushed with 20:80 N_2:CO_2 gas mix) with 20 mM acetate as electron donor, 40 mM fumarate as electron acceptor was used to grow liquid cultures from colony picks. For metal reduction assays, 20 mM acetate was added with either 55 mM Fe(III) citrate, ~20 mM birnessite (Mn(IV)-oxide), or ~70 mM Fe(III)-oxide freshly precipitated from $FeCl_2$ by addition of NaOH and incubation at pH 7 for 1 h before washing in DI water. Fe(III)-oxide medium contained an increased concentration of 0.6 g/L $NaH_2PO_4H_2O$ to prevent further crystallization of the metal after autoclaving. All experiments were carried out at 30°C.

Deletion and complementation construction

Putative conduits were identified through a genomic search for gene clusters containing loci predicted to encode a β-barrel using PRED-TMBB (49), contiguous to periplasmic and extracellular multiheme *c*-type cytochromes or other redox proteins. Localization was predicted by comparing PSORT (48) and the presence/absence of lipid attachment sites (50). Constructs to delete each gene cluster were designed to recombine to leave the site marker-free and also non-polar when located in larger transcriptional units, with

most primers and plasmids for the single deletions described in Chan *et al.*, 2017. When genes were part of a larger transcriptional unit or contained an upstream promoter, it was left intact. For example, in the case of the *omcBC* cluster the transcriptional regulator *orfR* (GSU2741) was left intact, and in *extEFG* the promoter and untranslated region was left intact so as to not disrupt the downstream loci.

For deletion mutant construction, the suicide vector pK18*mobsacB* (83) with ~750 bp flanking to the target region was used to induce homologous recombination as previously described (56). Briefly, two rounds of homologous recombination were selected for. The first selection used kanamycin resistance to select for mutants with the plasmid inserted into either up or downstream regions, and the second selection used sucrose sensitivity to select for mutants that recombine the plasmid out of the chromosome, resulting in either wild type or complete deletion mutants. Deletion mutants were identified using a kanamycin sensitivity test and verified by PCR amplification targeting the region. Multiple PCR amplifications with primers in different regions were used to confirm full deletion of each gene cluster (55 and Table S1).

During this work, we found that manipulations in the *omcBC* cluster, which harbors large regions of 100% identity, frequently underwent recombination into unexpected hybrid mutants which could escape routine PCR verification. For example, when *omaB* and *omaC* genes recombined, a large hybrid operon containing *omaB* linked to *ombC-omc*C would result, and sometimes the region would recombine to produce a hybrid of te two repressors controlling expression of the region. Routine primer screening, especially

targeting flanking regions, failed to detect the large product. Only via use of multiple internal primers (55 and Table S1), paired with longer-read or single molecule (PacBio) sequencing, were we able to verify and isolate strains in which complete loss of the *omcBC* cluster occurred, and dispose of hybrid mutants. Whole-genome resequencing was also performed on strains containing only one cluster, such as the strain containing only *extABCD*, especially since this strain has an unexpected phenotype where it produced more current than wild type. Because these hybrid *omcBC* operon strains still contained mixed conduits and had altered expression due to disruption of the repressors upstream, verification by PCR and whole genome sequencing (especially with single-molecule techniques able to span the entire ~10 kb region) are recommended to confirm deletions of large and repetitive regions such as the *omcBC* cluster when working with this region.

Mutants lacking a single gene region were used as parent strains to build additional mutations. In this manner, six double gene-cluster deletion mutants, four triple-cluster deletion mutants and one quintuple-cluster deletion mutant lacking up to nineteen genes were constructed (Fig. 1; Table 1). For complementation strains, putative conduits were amplified using primers listed in Table S1 and inserted into the *G. sulfurreducens* expression vector pRK2-Geo2 (56), which contains a constitutive promoter P_{acpP}. The putative conduit *extABCD* was assembled into a single transcriptional unit to ensure expression.

Electrode reduction assays

Sterile three-electrode conical reactors containing 15 mL of NB with 40 mM acetate as electron donor and 50 mM NaCl to equilibrate salt concentration were flushed with a mix of N_2-CO_2 gas (80:20, v/v) until the O_2 concentration reached less than 2 ppm. Liquid cultures were prepared by inoculating 1 ml liquid cultures from single colonies inside an anaerobic chamber. Once these cultures reached late exponential to stationary phase, they were used to inoculate 10 ml cultures with 10% v/v. Each reactor was then inoculated with 25% v/v from this liquid culture as it approached acceptor limitation, at an OD_{600} between 0.48 and 0.52. Working electrodes were set at either -0.1 V or +0.24 V vs SHE and average current density recorded every 12 seconds. Each liquid culture propagated from an individual colony pick served no more than two reactors, and at least three separate colonies were picked for all electrode reduction experiments for a final $n \geq 3$.

Metal reduction assays

NB medium with 20 mM acetate as electron donor and either 55 mM Fe(III)-citrate, ~70 mM Fe(III) oxide, or ~20 mM birnessite ($Mn(IV)O_2$) as electron acceptor was inoculated with a 0.1% inoculum of early stationary phase fumarate limited cultures. Time points were taken as necessary with anaerobic and sterile needles. These were diluted 1:10 into 0.5 N HCl for the Fe(III) samples and into 2 N HCl, 4 mM $FeSO_4$ for Mn(IV) samples. Samples were diluted once more by 1:10 in the case of Fe(III) assays and by 1:5 in the case of Mn(IV) assays into 0.5 N HCl. FerroZine^R reagent was then used to determine the Fe(II) concentration in each sample. Original Fe(II) concentrations were calculated for Fe(III) reduction assays by accounting for dilutions and original Mn(IV)

726 concentrations were calculated by accounting for the concentration of Fe(II) oxidized by
727 Mn(IV) based on the following: Mn(IV) + 2Fe(II) = Mn(II) + 2Fe(III). In other words, two
728 molecules of Fe(II) are reduced by one molecule of Mn(IV). Therefore, the increase of
729 Fe(II) concentration over time in our samples indicates a decrease of Mn(IV), or
730 increase of Mn(II), in a 2:1 ratio.
731
732 *RNAseq*
733 For liquid-grown cultures, total RNA was extracted from 10 ml of *G.*
734 *sulfurreducens* culture grown to mid-log (0.25 – 0.3 OD_{600}). For biofilm-grown cultures,
735 total RNA was extracted from graphite electrodes of *G. sulfurreducens* biofilms grown to
736 mid-log (300 μA/cm^2). Biofilms were rinsed to remove planktonic cells and removed
737 from electrodes using a plastic spatula. Cell pellets from all samples were washed in
738 RNAprotect (Qiagen) and frozen at -80°C before RNA extraction using RNeasy with on
739 column DNase treatment (Qiagen). Ribosomal RNA was depleted using RiboZero
740 (Illumina) by the University of Minnesota Genomics Center before stranded synthesis
741 and sequenced on Illumina HiSeq 2500, 125 bp pair-ended mode. Residual ribosomal
742 RNA sequences were removed before analysis using Rockhopper (84). Duplicate
743 biological samples were analyzed for each strain. An in-house re-sequenced *G.*
744 *sulfurreducens* genome and annotation released in a prior publication was used as
745 reference (46, 56). Full RPKM values are in Table S2, and raw RNAseq reads are
746 deposited in the NCBI SRA under our BioProject PRJNA290373.
747
748 *Homolog search and alignment*

749 Homologs to each of the individual cytochrome conduit proteins were queried on 11-30-
750 2016 in the Integrated Microbial Genomes database (85) with a cutoff on 75% sequence
751 length and 40% identity based on amino acid sequence within the Desulfuromonadales.
752 A higher percent identity was demanded in this search due to the high heme binding
753 site density with the invariable CXXCH sequence. Only ExtJ and ExtL were excluded
754 from the search and the OmcBC region was collapsed into a single cluster due to the
755 high identity shared between the two copies. The gene neighborhood around each
756 homolog hit was analyzed. With a few exceptions (see Table S2), all homologs were
757 found to be conserved in gene clusters predicted to encode cytochrome conduits and
758 containing several additional homologs to each corresponding *G. sulfurreducens*
759 conduit. The proteins within each homologous cytochrome conduit that did not fall within
760 the set cutoff were aligned to the amino acid sequence of the *G. sulfurreducens*
761 component they replaced using ClustalΩ (86).

762 **ACKNOWLEDGEMENTS**

763 We thank J. Badalamenti for sequence analysis assistance and data management. This
764 research was supported by the Office of Naval Research (N000141210308). FJO is
765 supported by the National Council of Science and Technology of Mexico (CONACYT).

766

REFERENCES

1. Tadanier CJ, Schreiber ME, Roller JW. 2005. Arsenic mobilization through microbially mediated deflocculation of ferrihydrite. Environ Sci Technol 39:3061–3068.

2. N'Guessan AL, Vrionis HA, Resch CT, Long PE, Lovley DR. 2008. Sustained removal of uranium from contaminated groundwater following stimulation of dissimilatory metal reduction. Environ Sci Technol 42:2999–3004.

3. Toner BM, Fakra SC, Manganini SJ, Santelli CM, Marcus MA, Moffett JW, Rouxel O, German CR, Edwards KJ. 2009. Preservation of iron(II) by carbon-rich matrices in a hydrothermal plume. Nat Geosci 2:197–201.

4. Williams KH, Long PE, Davis JA, Wilkins MJ, N'Guessan AL, Steefel CI, Yang L, Newcomer D, Spane FA, Kerkhof LJ, McGuinness L, Dayvault R, Lovley DR. 2011. Acetate availability and its influence on sustainable bioremediation of uranium-contaminated groundwater. Geomicrobiol J 28:519–539.

5. Yelton AP, Williams KH, Fournelle J, Wrighton KC, Handley KM, Banfield JF. 2013. Vanadate and acetate biostimulation of contaminated sediments decreases diversity, selects for specific taxa, and decreases aqueous V5+ soncentration. Environ Sci Technol 47:6500–6509.

6. Couture R-M, Charlet L, Markelova E, Madé B, Parsons CT. 2015. On–off mobilization of contaminants in soils during redox oscillations. Environ Sci Technol 49:3015–3023.

7. Bond DR, Holmes DE, Tender LM, Lovley DR. 2002. Electrode-reducing microorganisms that harvest energy from marine sediments. Science 295:483–485.

788 8. Bond DR, Lovley DR. 2003. Electricity production by *Geobacter sulfurreducens* attached to
789 electrodes. Appl Environ Microbiol 69:1548–1555.

790 9. Holmes DE, Bond DR, O'Neil RA, Reimers CE, Tender LR, Lovley DR. 2004. Microbial
791 communities associated with electrodes harvesting electricity from a variety of aquatic
792 sediments. Microb Ecol 48:178–190.

793 10. Ren Z, Steinberg LM, Regan JM. 2008. Electricity production and microbial biofilm
794 characterization in cellulose-fed microbial fuel cells. Water Sci Technol 58:617–622.

795 11. Logan BE, Rabaey K. 2012. Conversion of wastes into bioelectricity and chemicals by
796 using microbial electrochemical technologies. Science 337:686–690.

797 12. Schrader PS, Reimers CE, Girguis P, Delaney J, Doolan C, Wolf M, Green D. 2016.
798 Independent benthic microbial fuel cells powering sensors and acoustic communications
799 with the MARS underwater observatory. J Atmospheric Ocean Technol 33:607–617.

800 13. Schievano A, Pepé Sciarria T, Vanbroekhoven K, De Wever H, Puig S, Andersen SJ,
801 Rabaey K, Pant D. 2016. Electro-fermentation – Merging electrochemistry with
802 fermentation in industrial applications. Trends Biotechnol 34:866–878.

803 14. Gralnick JA, Newman DK. 2007. Extracellular respiration. Mol Microbiol 65:1–11.

804 15. Shi L, Dong H, Reguera G, Beyenal H, Lu A, Liu J, Yu H-Q, Fredrickson JK. 2016.
805 Extracellular electron transfer mechanisms between microorganisms and minerals. Nat
806 Rev Microbiol 14:651–662.

807 16. Navrotsky A, Mazeina L, Majzlan J. 2008. Size-driven structural and thermodynamic
808 complexity in iron oxides. Science 319:1635–1638.

17. Majzlan J. 2013. Minerals and aqueous species of iron and manganese as reactants and products of microbial metal respiration, p. 1–28. *In* Gescher, J, Kappler, A (eds.), Microbial Metal Respiration. Springer Berlin Heidelberg.

18. Levar CE, Hoffman CL, Dunshee AJ, Toner BM, Bond DR. 2017. Redox potential as a master variable controlling pathways of metal reduction by *Geobacter sulfurreducens*. ISME J 11:741–752.

19. Marsili E, Sun J, Bond DR. 2010. Voltammetry and growth physiology of *Geobacter sulfurreducens* biofilms as a function of growth stage and imposed electrode potential. Electroanalysis 22:865–874.

20. Snider RM, Strycharz-Glaven SM, Tsoi SD, Erickson JS, Tender LM. 2012. Long-range electron transport in *Geobacter sulfurreducens* biofilms is redox gradient-driven. Proc Natl Acad Sci 109:15467–15472.

21. Robuschi L, Tomba JP, Schrott GD, Bonanni PS, Desimone PM, Busalmen JP. 2013. Spectroscopic slicing to reveal internal redox gradients in electricity-producing biofilms. Angew Chem Int Ed 52:925–928.

22. Zacharoff L, Chan CH, Bond DR. 2016. Reduction of low potential electron acceptors requires the CbcL inner membrane cytochrome of *Geobacter sulfurreducens*. Bioelectrochemistry 107:7–13.

23. Levar CE, Chan CH, Mehta-Kolte MG, Bond DR. 2014. An inner membrane cytochrome required only for reduction of high redox potential extracellular electron acceptors. mBio 5:e02034-14.

24. Nevin KP, Kim B-C, Glaven RH, Johnson JP, Woodard TL, Methé BA, Jr RJD, Covalla SF, Franks AE, Liu A, Lovley DR. 2009. Anode biofilm transcriptomics reveals outer surface components essential for high density current production in *Geobacter sulfurreducens* fuel cells. PLOS ONE 4:e5628.

25. Leang C, Qian X, Mester T, Lovley DR. 2010. Alignment of the *c*-type cytochrome OmcS along pili of *Geobacter sulfurreducens*. Appl Environ Microbiol 76:4080–4084.

26. Tremblay P-L, Summers ZM, Glaven RH, Nevin KP, Zengler K, Barrett CL, Qiu Y, Palsson BO, Lovley DR. 2011. A *c*-type cytochrome and a transcriptional regulator responsible for enhanced extracellular electron transfer in *Geobacter sulfurreducens* revealed by adaptive evolution. Environ Microbiol 13:13–23.

27. Qian X, Mester T, Morgado L, Arakawa T, Sharma ML, Inoue K, Joseph C, Salgueiro CA, Maroney MJ, Lovley DR. 2011. Biochemical characterization of purified OmcS, a *c*-type cytochrome required for insoluble Fe(III) reduction in *Geobacter sulfurreducens*. Biochim Biophys Acta BBA - Bioenerg 1807:404–412.

28. Smith JA, Tremblay P-L, Shrestha PM, Snoeyenbos-West OL, Franks AE, Nevin KP, Lovley DR. 2014. Going wireless: Fe(III) oxide reduction without pili by *Geobacter sulfurreducens* strain JS-1. Appl Environ Microbiol 80:4331–4340.

29. Peng L, Zhang Y. 2017. Cytochrome OmcZ is essential for the current generation by *Geobacter sulfurreducens* under low electrode potential. Electrochimica Acta 228:447–452.

30. Zacharoff LA, Morrone D, Bond DR. 2017. *Geobacter sulfurreducens* extracellular multiheme cytochrome PgcA facilitates respiration to Fe(III) oxides but not electrodes. Front Microbiol 8:2481.

853 31. Reguera G, Nevin KP, Nicoll JS, Covalla SF, Woodard TL, Lovley DR. 2006. Biofilm and
854 nanowire production leads to increased current in *Geobacter sulfurreducens* fuel cells.
855 Appl Environ Microbiol 72:7345–7348.

856 32. Richardson DJ, Butt JN, Fredrickson JK, Zachara JM, Shi L, Edwards MJ, White G, Baiden
857 N, Gates AJ, Marritt SJ, Clarke TA. 2012. The “porin–cytochrome” model for microbe-to-
858 mineral electron transfer. Mol Microbiol 85:201–212.

859 33. Shi L, Fredrickson JK, Zachara JM. 2014. Genomic analyses of bacterial porin-cytochrome
860 gene clusters. Front Microbiol 5:657.

861 34. Liu Y, Wang Z, Liu J, Levar C, Edwards MJ, Babauta JT, Kennedy DW, Shi Z, Beyenal H,
862 Bond DR, Clarke TA, Butt JN, Richardson DJ, Rosso KM, Zachara JM, Fredrickson JK, Shi
863 L. 2014. A trans-outer membrane porin-cytochrome protein complex for extracellular
864 electron transfer by *Geobacter sulfurreducens* PCA. Environ Microbiol Rep 6:776–785.

865 35. Hartshorne RS, Reardon CL, Ross D, Nuester J, Clarke TA, Gates AJ, Mills PC,
866 Fredrickson JK, Zachara JM, Shi L, Beliaev AS, Marshall MJ, Tien M, Brantley S, Butt JN,
867 Richardson DJ. 2009. Characterization of an electron conduit between bacteria and the
868 extracellular environment. Proc Natl Acad Sci 106:22169–22174.

869 36. Wang Z, Liu C, Wang X, Marshall MJ, Zachara JM, Rosso KM, Dupuis M, Fredrickson JK,
870 Heald S, Shi L. 2008. Kinetics of reduction of Fe(III) complexes by outer membrane
871 cytochromes MtrC and OmcA of *Shewanella oneidensis* MR-1. Appl Environ Microbiol
872 74:6746–6755.

873 37. Coursolle D, Gralnick JA. 2012. Reconstruction of extracellular respiratory pathways for
874 iron(III) reduction in *Shewanella oneidensis* strain MR-1. Front Microbiol 3.

875 38. White GF, Shi Z, Shi L, Wang Z, Dohnalkova AC, Marshall MJ, Fredrickson JK, Zachara
876 JM, Butt JN, Richardson DJ, Clarke TA. 2013. Rapid electron exchange between surface-
877 exposed bacterial cytochromes and Fe(III) minerals. Proc Natl Acad Sci 110:6346–6351.

878 39. Baron D, LaBelle E, Coursolle D, Gralnick JA, Bond DR. 2009. Electrochemical
879 measurement of electron transfer kinetics by *Shewanella oneidensis* MR-1. J Biol Chem
880 284:28865–28873.

881 40. Coursolle D, Baron DB, Bond DR, Gralnick JA. 2010. The Mtr respiratory pathway is
882 essential for reducing flavins and electrodes in *Shewanella oneidensis*. J Bacteriol
883 192:467–474.

884 41. Gralnick JA, Vali H, Lies DP, Newman DK. 2006. Extracellular respiration of dimethyl
885 sulfoxide by *Shewanella oneidensis* strain MR-1. Proc Natl Acad Sci U S A 103:4669–
886 4674.

887 42. Jiao Y, Newman DK. 2007. The *pio* operon is essential for phototrophic Fe(II) oxidation in
888 *Rhodopseudomonas palustris* TIE-1. J Bacteriol 189:1765–1773.

889 43. Leang C, Coppi MV, Lovley DR. 2003. OmcB, a *c*-type polyheme cytochrome, involved in
890 Fe(III) reduction in *Geobacter sulfurreducens*. J Bacteriol 185:2096–2103.

891 44. Leang C, Lovley DR. 2005. Regulation of two highly similar genes, *omcB* and *omcC*, in a
892 10 kb chromosomal duplication in *Geobacter sulfurreducens*. Microbiology 151:1761–
893 1767.

894 45. Liu Y, Fredrickson JK, Zachara JM, Shi L. 2015. Direct involvement of *ombB*, *omaB*, and
895 *omcB* genes in extracellular reduction of Fe(III) by *Geobacter sulfurreducens* PCA. Front
896 Microbiol 1075.

897 46. Chan CH, Levar CE, Jiménez Otero F, Bond DR. 2017. Genome scale mutational analysis
898 of *Geobacter sulfurreducens* reveals distinct molecular mechanisms for respiration and
899 sensing of poised electrodes vs. Fe(III) oxides. J Bacteriol 119:e00340-17.

900 47. Jiménez Otero F, Bond DR. 2017. Gene clusters encoding putative outer membrane
901 electron conduits have specific roles during metal and electrode respiration in *Geobacter*
902 *sulfurreducens*. bioRxiv 169086.

903 48. Yu NY, Wagner JR, Laird MR, Melli G, Rey S, Lo R, Dao P, Sahinalp SC, Ester M, Foster
904 LJ, Brinkman FSL. 2010. PSORTb 3.0: improved protein subcellular localization prediction
905 with refined localization subcategories and predictive capabilities for all prokaryotes.
906 Bioinformatics 26:1608–1615.

907 49. Bagos PG, Liakopoulos TD, Spyropoulos IC, Hamodrakas SJ. 2004. PRED-TMBB: a web
908 server for predicting the topology of β-barrel outer membrane proteins. Nucleic Acids Res
909 32:W400–W404.

910 50. Juncker AS, Willenbrock H, von Heijne G, Brunak S, Nielsen H, Krogh A. 2003. Prediction
911 of lipoprotein signal peptides in Gram-negative bacteria. Protein Sci Publ Protein Soc
912 12:1652–1662.

913 51. Aklujkar M, Coppi MV, Leang C, Kim BC, Chavan MA, Perpetua LA, Giloteaux L, Liu A,
914 Holmes DE. 2013. Proteins involved in electron transfer to Fe(III) and Mn(IV) oxides by
915 *Geobacter sulfurreducens* and *Geobacter uraniireducens*. Microbiology 159:515–535.

916 52. Fujita M, Mihara H, Goto S, Esaki N, Kanehisa M. 2007. Mining prokaryotic genomes for
917 unknown amino acids: a stop-codon-based approach. BMC Bioinformatics 8:225.

53. Coursolle D, Gralnick JA. 2010. Modularity of the Mtr respiratory pathway of *Shewanella oneidensis* strain MR-1. Mol Microbiol 77:995–1008.

54. Clarke TA, Edwards MJ, Gates AJ, Hall A, White GF, Bradley J, Reardon CL, Shi L, Beliaev AS, Marshall MJ, Wang Z, Watmough NJ, Fredrickson JK, Zachara JM, Butt JN, Richardson DJ. 2011. Structure of a bacterial cell surface decaheme electron conduit. Proc Natl Acad Sci 108:9384–9389.

55. Edwards MJ, Hall A, Shi L, Fredrickson JK, Zachara JM, Butt JN, Richardson DJ, Clarke TA. 2012. The crystal structure of the extracellular 11-heme cytochrome UndA reveals a conserved 10-heme motif and defined binding site for soluble iron chelates. Structure 20:1275–1284.

56. Chan CH, Levar CE, Zacharoff L, Badalamenti JP, Bond DR. 2015. Scarless genome editing and stable inducible expression vectors for *Geobacter sulfurreducens*. Appl Environ Microbiol 81:7178–7186.

57. Holmes DE, Chaudhuri SK, Nevin KP, Mehta T, Methé BA, Liu A, Ward JE, Woodard TL, Webster J, Lovley DR. 2006. Microarray and genetic analysis of electron transfer to electrodes in *Geobacter sulfurreducens*. Environ Microbiol 8:1805–1815.

58. Bonanni PS, Bradley DF, Schrott GD, Busalmen JP. 2013. Limitations for current production in *Geobacter sulfurreducens* biofilms. ChemSusChem 6:711–720.

59. Juárez K, Kim B-C, Nevin K, Olvera L, Reguera G, Lovley DR, Methé BA. 2009. PilR, a transcriptional regulator for pilin and other genes required for Fe(III) reduction in *Geobacter sulfurreducens*. J Mol Microbiol Biotechnol 16:146–158.

939 60. Steidl RJ, Lampa-Pastirk S, Reguera G. 2016. Mechanistic stratification in electroactive
940 biofilms of *Geobacter sulfurreducens* mediated by pilus nanowires. Nat Commun 7:12217.

941 61. Kim B-C, Leang C, Ding Y-HR, Glaven RH, Coppi MV, Lovley DR. 2005. OmcF, a putative
942 *c*-type monoheme outer membrane cytochrome required for the expression of other outer
943 membrane cytochromes in *Geobacter sulfurreducens*. J Bacteriol 187:4505–4513.

944 62. Methé BA, Nelson KE, Eisen JA, Paulsen IT, Nelson W, Heidelberg JF, Wu D, Wu M,
945 Ward N, Beanan MJ, Dodson RJ, Madupu R, Brinkac LM, Daugherty SC, DeBoy RT,
946 Durkin AS, Gwinn M, Kolonay JF, Sullivan SA, Haft DH, Selengut J, Davidsen TM, Zafar N,
947 White O, Tran B, Romero C, Forberger HA, Weidman J, Khouri H, Feldblyum TV,
948 Utterback TR, Aken SEV, Lovley DR, Fraser CM. 2003. Genome of *Geobacter*
949 *sulfurreducens:* metal reduction in subsurface environments. Science 302:1967–1969.

950 63. Shelobolina ES, Coppi MV, Korenevsky AA, DiDonato LN, Sullivan SA, Konishi H, Xu H,
951 Leang C, Butler JE, Kim B-C, Lovley DR. 2007. Importance of *c*-type cytochromes for
952 U(VI) reduction by *Geobacter sulfurreducens*. BMC Microbiol 7:16.

953 64. Richter H, P. Nevin K, Jia H, A. Lowy D, R. Lovley D, M. Tender L. 2009. Cyclic
954 voltammetry of biofilms of wild type and mutant *Geobacter sulfurreducens* on fuel cell
955 anodes indicates possible roles of OmcB, OmcZ, type IV pili, and protons in extracellular
956 electron transfer. Energy Environ Sci 2:506–516.

957 65. Stephen CS, LaBelle EV, Brantley SL, Bond DR. 2014. Abundance of the multiheme *c*-
958 type cytochrome OmcB increases in outer biofilm layers of electrode-grown *Geobacter*
959 *sulfurreducens*. PLOS ONE 9:e104336.

960 66. Ueki T, DiDonato LN, Lovley DR. 2017. Toward establishing minimum requirements for
961 extracellular electron transfer in *Geobacter sulfurreducens*. FEMS Microbiol Lett 364.

962 67. Butler JE, Kaufmann F, Coppi MV, Núñez C, Lovley DR. 2004. MacA, a diheme *c*-type
963 cytochrome involved in Fe(III) reduction by *Geobacter sulfurreducens*. J Bacteriol
964 186:4042–4045.

965 68. Kim B-C, Lovley DR. 2008. Investigation of direct vs. indirect involvement of the *c*-type
966 cytochrome MacA in Fe(III) reduction by *Geobacter sulfurreducens*. FEMS Microbiol Lett
967 286:39–44.

968 69. Seidel J, Hoffmann M, Ellis KE, Seidel A, Spatzal T, Gerhardt S, Elliott SJ, Einsle O. 2012.
969 MacA is a second cytochrome *c* peroxidase of *Geobacter sulfurreducens*. Biochemistry
970 (Mosc) 51:2747–2756.

971 70. Gennaris A, Ezraty B, Henry C, Agrebi R, Vergnes A, Oheix E, Bos J, Leverrier P,
972 Espinosa L, Szewczyk J, Vertommen D, Iranzo O, Collet J-F, Barras F. 2015. Repairing
973 oxidized proteins in the bacterial envelope using respiratory chain electrons. Nature
974 528:409–412.

975 71. Appel J, Phunpruch S, Steinmüller K, Schulz R. 2000. The bidirectional hydrogenase of
976 *Synechocystis sp.* PCC 6803 works as an electron valve during photosynthesis. Arch
977 Microbiol 173:333–338.

978 72. Coppi MV. 2005. The hydrogenases of *Geobacter sulfurreducens*: a comparative genomic
979 perspective. Microbiology 151:1239–1254.

980 73. Qiu Y, Cho B-K, Park YS, Lovley D, Palsson BØ, Zengler K. 2010. Structural and
981 operational complexity of the *Geobacter sulfurreducens* genome. Genome Res 20:1304–
982 1311.

983 74. Aussignargues C, Giuliani M-C, Infossi P, Lojou E, Guiral M, Giudici-Orticoni M-T, Ilbert M.
984 2012. Rhodanese functions as sulfur supplier for key enzymes in sulfur energy
985 metabolism. J Biol Chem 287:19936–19948.

986 75. Prat L, Maillard J, Rohrbach-Brandt E, Holliger C. 2012. An unusual tandem-domain
987 rhodanese harbouring two active sites identified in *Desulfitobacterium hafniense*. FEBS J
988 279:2754–2767.

989 76. Ravot G, Casalot L, Ollivier B, Loison G, Magot M. 2005. *rdlA*, a new gene encoding a
990 rhodanese-like protein in *Halanaerobium congolense* and other thiosulfate-reducing
991 anaerobes. Res Microbiol 156:1031–1038.

992 77. Ramírez P, Toledo H, Guiliani N, Jerez CA. 2002. An exported rhodanese-like protein is
993 induced during growth of *Acidithiobacillus ferrooxidans* in metal sulfides and different sulfur
994 compounds. Appl Environ Microbiol 68:1837–1845.

995 78. Jahan MI, Tobe R, Mihara H. 2018. Characterization of a novel porin-like protein, ExtI,
996 from *Geobacter sulfurreducens* and its implication in the reduction of Selenite and Tellurite.
997 Int J Mol Sci 19:809.

998 79. Nelson CE, Rogowski A, Morland C, Wilhide JA, Gilbert HJ, Gardner JG. 2017. Systems
999 analysis in *Cellvibrio japonicus* resolves predicted redundancy of β-glucosidases and
1000 determines essential physiological functions. Mol Microbiol 104:294–305.

1001 80. Cutting RS, Coker VS, Fellowes JW, Lloyd JR, Vaughan DJ. 2009. Mineralogical and
1002 morphological constraints on the reduction of Fe(III) minerals by *Geobacter*
1003 *sulfurreducens*. Geochim Cosmochim Acta 73:4004–4022.

1004 81. Coker VS, Byrne JM, Telling ND, Van Der Laan G, Lloyd JR, Hitchcock AP, Wang J,
1005 Pattrick R a. D. 2012. Characterisation of the dissimilatory reduction of Fe(III)-
1006 oxyhydroxide at the microbe – mineral interface: the application of STXM–XMCD.
1007 Geobiology 10:347–354.

1008 82. Eusterhues K, Hädrich A, Neidhardt J, Küsel K, Keller TF, Jandt KD, Totsche KU. 2014.
1009 Reduction of ferrihydrite with adsorbed and coprecipitated organic matter: microbial
1010 reduction by *Geobacter bremensis* vs. abiotic reduction by Na-dithionite. Biogeosciences
1011 11:4953–4966.

1012 83. Simon R, Priefer U, Pühler A. 1983. A broad host range mobilization system for in vivo
1013 genetic engineering: Transposon mutagenesis in Gram negative bacteria. Nat Biotechnol
1014 1:784–791.

1015 84. McClure R, Balasubramanian D, Sun Y, Bobrovskyy M, Sumby P, Genco CA, Vanderpool
1016 CK, Tjaden B. 2013. Computational analysis of bacterial RNA-Seq data. Nucleic Acids Res
1017 41:e140–e140.

1018 85. Markowitz VM, Chen I-MA, Palaniappan K, Chu K, Szeto E, Grechkin Y, Ratner A, Jacob
1019 B, Huang J, Williams P, Huntemann M, Anderson I, Mavromatis K, Ivanova NN, Kyrpides
1020 NC. 2012. IMG: the integrated microbial genomes database and comparative analysis
1021 system. Nucleic Acids Res 40:D115–D122.

1022 86. Sievers F, Wilm A, Dineen D, Gibson TJ, Karplus K, Li W, Lopez R, McWilliam H,
1023 Remmert M, Söding J, Thompson JD, Higgins DG. 2011. Fast, scalable generation of high-
1024 quality protein multiple sequence alignments using Clustal Omega. Mol Syst Biol 7:539.

Tables:

Table 1

Strains and Plasmids	Description or relevant genotype	Reference
Geobacter sulfurreducens strains		
DB1279	ΔGSU2731-39 (Δ*omcBC*)	Chan *et al*., 2017
DB1280	ΔGSU2645-42 (Δ*extABCD*)	Chan *et al*., 2017
DB1281	ΔGSU2940-36 (Δ*extHIJKL*)	Chan *et al*., 2017
DB1282	ΔGSU2724-26 (Δ*extEFG*)	Chan *et al*., 2017
DB1487	ΔGSU2731-39 ΔGSU2645-42 (Δ*omcBC* Δ*extABCD*)	This study
DB1488	ΔGSU2731-39 ΔGSU2724-26 (Δ*omcBC* Δ*extEFG*)	This study
DB1289	ΔGSU2731-39 ΔGSU2940-36 (Δ*omcBC* Δ*extHIJKL*)	This study
DB1489	ΔGSU2645-42 ΔGSU2724-26 (Δ*extABCD* Δ*extEFG*)	This study
DB1490	ΔGSU2645-42 ΔGSU2940-36 (Δ*extABCD* Δ*extHIJKL*)	This study
DB1290	ΔGSU2731-39 ΔGSU2940-36 ΔGSU2724-26 (*extABCD*$^{+}$)	This study
DB1291	ΔGSU2731-39 ΔGSU2645-42 ΔGSU2936-2940 (*extEFG*$^{+}$)	This study
DB1491	ΔGSU2731-39 ΔGSU2645-42 ΔGSU2726-24 (*extHIJKL*$^{+}$)	This study
DB1492	ΔGSU2645-42 ΔGSU2726-24 Δ2940-36 (*omcBC*$^{+}$)	This study
DB1493	ΔGSU2731-39 ΔGSU2645-42 ΔGSU2726-24 ΔGSU2940-36 (Δ5)	This study
Escherichia coli		
S17-1	*recA pro hsdR* RP4-2-Tc::Mu-Km::Tn7	Simon *et al.*, 1983
Plasmids		
pK18*mobsacB*		Simon *et al*., 1983
pRK2-Geo2		Chan *et al*., 2015
p*DomcBC*	Flanking regions of *omcBC* in pK18*mobsacB*	This study
p*DextABCD*	Flanking regions of *extABCD* in pK18*mobsacB*	This study
p*DextEFG*	Flanking regions of *extEFG* in pK18*mobsacB*	This study
p*DextHIJKL*	Flanking regions of *extHIJKL* in pK18*mobsacB*	This study
p*omcB*	*ombB-omaB-omcB* in pRK2-Geo2	This study
p*extABCD*	*extABCD* in pRK2-Geo2	This study

Table 1. Strains and plasmids used in this study.

Table 2

	% of wild type								
Substrate	Δ*omcBC*	Δ*extABCD*	Δ*extEFG*	Δ*extHIJKL*	*omcBC*$^{+}$	*extABCD*$^{+}$	*extEFG*$^{+}$	*extHIJKL*$^{+}$	Δ5
Fe(III) citrate	61.2 ± 10.5	105 ± 6.6	62.5 ± 4.9	66.3 ± 2.5	101.1 ± 8.4	99.2 ± 11.3	22.5 ± 2.4	23.8 ± 6.4	0.1 ± 0.6
FeIII)-oxide	68.9 ± 8.4	83.3 ± 12.1	87.5 ± 14.9	95.8 ± 24.9	78.8 ± 3.9	29.2 ± 2.6	60.4 ± 9.5	52.1 ± 3.7	0.1 ± 0.3
Mn(IV)-oxide	94.5 ± 6.4	95.1 ± 2.8	99.6 ± 3.4	97.9 ± 6.1	83.3 ± 14.1	26.7 ± 5.9	86.8 ± 6.5	75.6 ± 7.3	1.7 ± 0.9
Electrode	76.5 ± 16.5	20.9 ± 6.0	104.8 ± 2.1	86.3 ± 15.3	28.3 ± 5.2	137.9 ± 9.5	21.2 ± 6.5	25.9 ± 4.2	21.9 ± 4.4

Table 2. Comparative performance of *G. sulfurreducens* strains lacking one cluster, or containing only one cluster. Growth of single cytochrome conduit deletion mutants and mutants lacking all clusters except one, averaged from eight biological replicates or more and represented as the percent of wild type growth. Averages and standard deviation represented.

Figure Legends

Figure 1. The outer membrane electron conduit gene clusters of *G. sulfurreducens*. A) Genetic organization and predicted features of operons containing putative outer membrane conduits. Deletion constructs indicated by dashed line. B) Identity matrix from amino acid sequence alignment of each cytochrome or ß-barrel component using ClustalΩ.

Figure 2. OmcBC or ExtABCD are sufficient during Fe(III)-citrate reduction, deletion of all clusters eliminates Fe(III)-citrate reduction. Growth using 55 mM Fe(III)-citrate as an electron acceptor by A) single conduit cluster deletion mutants, B) triple mutants lacking all but one cytochrome conduit, as well as the Δ5 strain lacking all five cytochrome conduits, C) mutants in an Δ*omcBC* background strain, and D) Δ5 mutants expressing *omcB* or *extABCD* or carrying an empty expression vector as control. All experiments were conducted in triplicate and curves are average ± SD of n ≥ 3 replicates.

Figure 3. No single outer membrane cluster is essential but all are necessary for wild type levels of electron transfer to Fe(III)- and Mn(IV)-oxides. Growth of single cluster deletion mutants and triple mutants lacking all but one cytochrome conduit cluster, as well as the Δ5 mutant lacking all clusters utilizing A-B) 70 mM Fe(III)-oxide or C-D) 20 mM Mn(IV)-oxide as terminal electron acceptor. All experiments were conducted in triplicate and curves are average ± SD of n ≥ 3 replicates.

Figure 4. OmcBC and ExtEFG have additive roles in Fe(III)- and Mn(IV)-oxide reduction. Reduction of A) 70 mM Fe(III)-oxide or B) 20 mM Mn(IV)-oxide by the Δ*omcBC* strain and additional deletions in an Δ*omcBC* background. All experiments were conducted in triplicate and curves are average ± SD of n ≥ 3 replicates.

Figure 5. Partial complementation by single conduit clusters supports hypothesis that multiple conduit complexes are necessary for wild-type levels of metal oxide reduction. Reduction of A) 70 mM Fe(III)-oxide or B) 20 mM Mn(IV)-oxide by the Δ5 mutant expressing *extABCD* or the *omcB* cluster compared to the empty vector control. All experiments were conducted in triplicate and curves are average ± SD of n ≥ 3 replicates.

Figure 6. Only the ExtABCD conduit cluster is necessary for electrode reduction. Current density produced by A) single and B) multiple-cluster deletion mutants on graphite electrodes poised at +0.24 V vs. SHE. All mutants were grown in at least two separate experiments, and curves are representative of n ≥ 3 independent replicates per experiment. Similar results were obtained at lower (-0.1 V vs. SHE) redox potentials.

Figure 7. Effect of kanamycin on final current density, and comparison of ExtABCD and OmcBC complementation. A) Final current density of wild type *G. sulfurreducens* compared to wild type carrying an empty vector in the presence of increasing kanamycin concentrations. B) Current density produced by the Δ5 strain plus

either *extABCD* or *omcB* cluster-containing vectors, in the presence of 5 μg/ml residual kanamycin. Wild type and Δ5 strains carrying the empty vector were used as controls. All experiments were conducted in duplicate and curves are representative of n ≥ 3 replicates per experiment.

Figure 8. Transcriptomic analysis comparing fumarate vs. electrode growth for *extABCD*$^{+}$ and wild type strains. A) Comparison of expression levels of wild type exponentially growing cells under fumarate- and electrode-respiring conditions, showing no significant up- or downregulation of *ext* clusters.(orange triangles) or most other known electron transfer proteins (red circles). Dark and light gray dotted lines represent thresholds of 4 and 2 Log_2, respectively. B) RPKM and Log_2 change of ORFs with largest expression changes as well as genes studied in this work (for additional data, see Table S2). Comparison of the transcriptome of wild type and *extABCD*$^{+}$ cells exponentially growing using C) fumarate or D) electrode poised at +240 mV as terminal electron acceptor, showing no changes to electron transfer proteins due to deletion of *omBC, extEFG,* and *extHIJKL* clusters. Averages shown of biological replicate samples.

Figure 9. Cytochrome conduit conservation across the Order Desulfuromonodales. Representation of cytochrome conduit clusters from the Desulfuromonodales with homologs to either A) OmcBC, B) ExtABCD, C) ExtEFG, or D) ExtHIJKL. Red arrows = putative outer membrane products with a predicted lipid attachment site, yellow arrows = predicted periplasmic components, green arrows = predicted outer membrane anchor components. Complete clusters with all components

sharing >40% identity to the corresponding *G. sulfurreducens* cytochrome conduit are indicated in boxes to the left of each gene cluster. Clusters in which one or more proteins are replaced by a new element with <40% identity are listed on the right side of each gene cluster. Proteins with numbers indicate the % identity to the *G. sulfurreducens* version.

[a]OmcBC homologs in these gene clusters also encode Hox hydrogenase complexes.

[b]Gene clusters have contiguous *extBCD* loci but *extA* is not in vicinity, as *extA* was found in separate parts of the genome for some of those organisms (see Supplemental Table S2). [c]Gene cluster has additional lipoprotein decaheme *c*-type cytochrome upstream of *extE*. [d]Lipid attachment sites corresponding to ExtJL could not be found but there is an additional small lipoprotein encoded within the gene cluster. For ExtHIJKL clusters, homologs depicted above *extH* are found in gene clusters containing only *extI*, whereas homologs depicted below *extH* are found in gene clusters containing full *extHIJKL* loci. Upstream and on the opposite strand to all gene clusters homologous to *extHIJKL* there is a transcription regulator of the LysR family, except [e], where there is no transcriptional regulator in that region, and [f], where there are transcriptional regulators of the TetR family instead.

Figure 1.

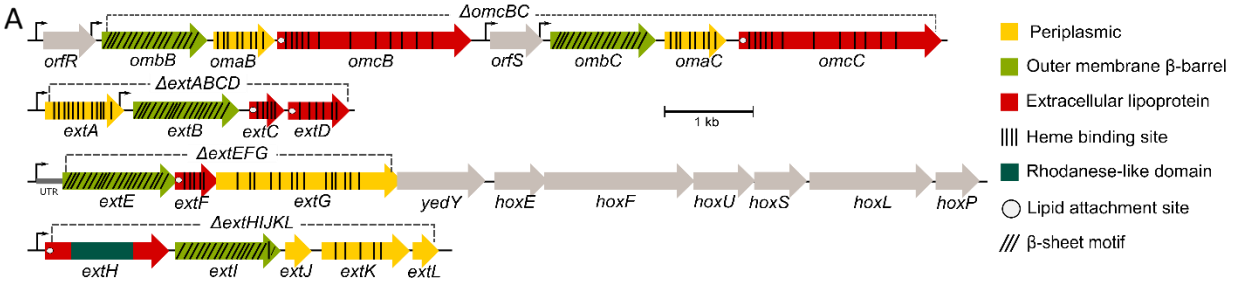

B

Percent Identity based on Amino Acid Sequence

Periplasmic cytochromes

	ExtA	ExtG	ExtK	OmaB	OmaC
ExtA	100	25.9	17.9	23.9	23.9
ExtG		100	20.9	23.2	23.2
ExtK			100	19.7	19.7
OmaB				100	100
OmaC					100

β-barrels

	ExtB	ExtE	ExtI	OmbB	OmbC
ExtB	100	30.2	21.1	22	22
ExtE		100	20.2	20.4	20.4
ExtI			100	17.1	17.1
OmbB				100	100
OmbC					100

Lipoprotein cytochromes

	ExtC	ExtD	ExtF	OmcB	OmcC
ExtC	100	16.3	41.5	21.2	24.2
ExtD		100	31.3	26.9	28.5
ExtF			100	22.9	23
OmcB				100	70.8
OmcC					100

Figure 1. The outer membrane electron conduit gene clusters of *G. sulfurreducens*. A) Genetic organization and predicted features of operons containing putative outer membrane conduits. Deletion constructs indicated by dashed line. B) Identity matrix from amino acid sequence alignment of each cytochrome or ß-barrel component using ClustalΩ.

Figure 2.

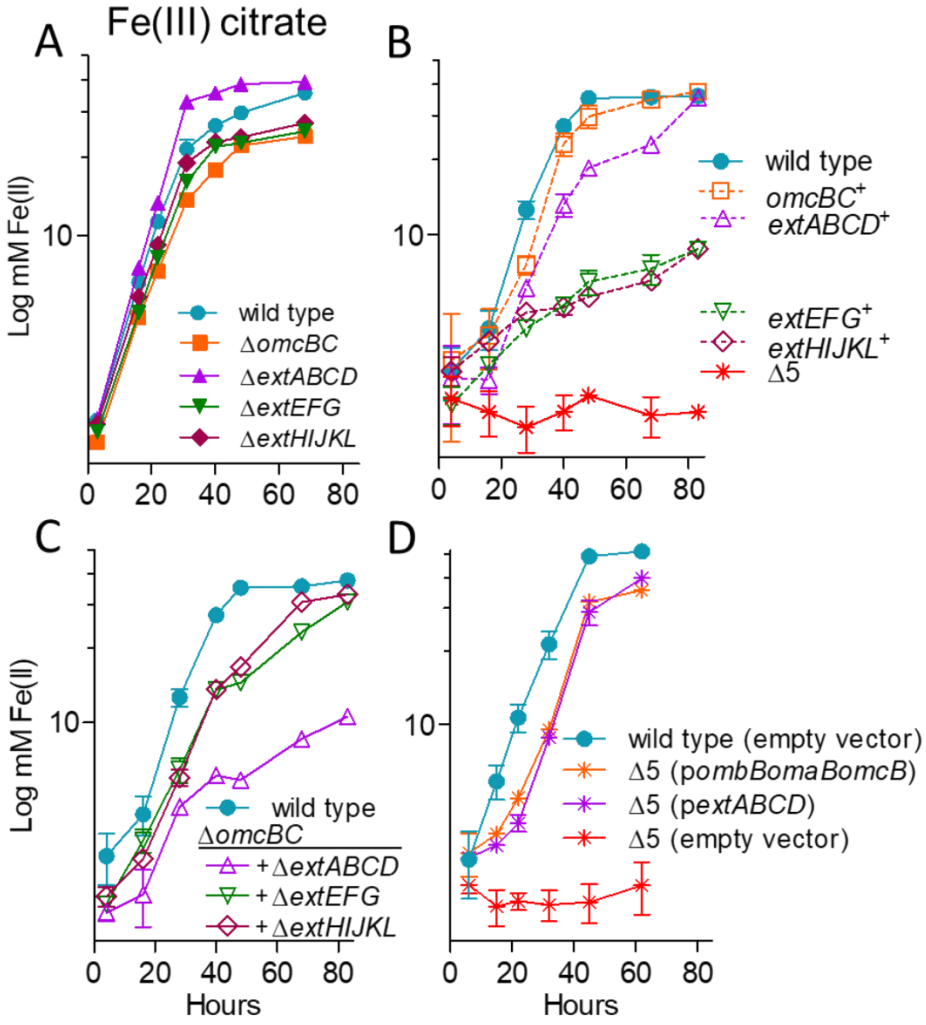

Figure 2. OmcBC or ExtABCD are sufficient during Fe(III)-citrate reduction, deletion of all clusters eliminates Fe(III)-citrate reduction. Growth using 55 mM Fe(III)-citrate as an electron acceptor by A) single conduit cluster deletion mutants, B) triple mutants lacking all but one cytochrome conduit, as well as the Δ5 strain lacking all five cytochrome conduits, C) mutants in an Δ*omcBC* background strain, and D) Δ5 mutants expressing *omcB* or *extABCD* or carrying an empty expression vector as control. All experiments were conducted in triplicate and curves are average ± SD of n ≥ 3 replicates.

Figure 3.

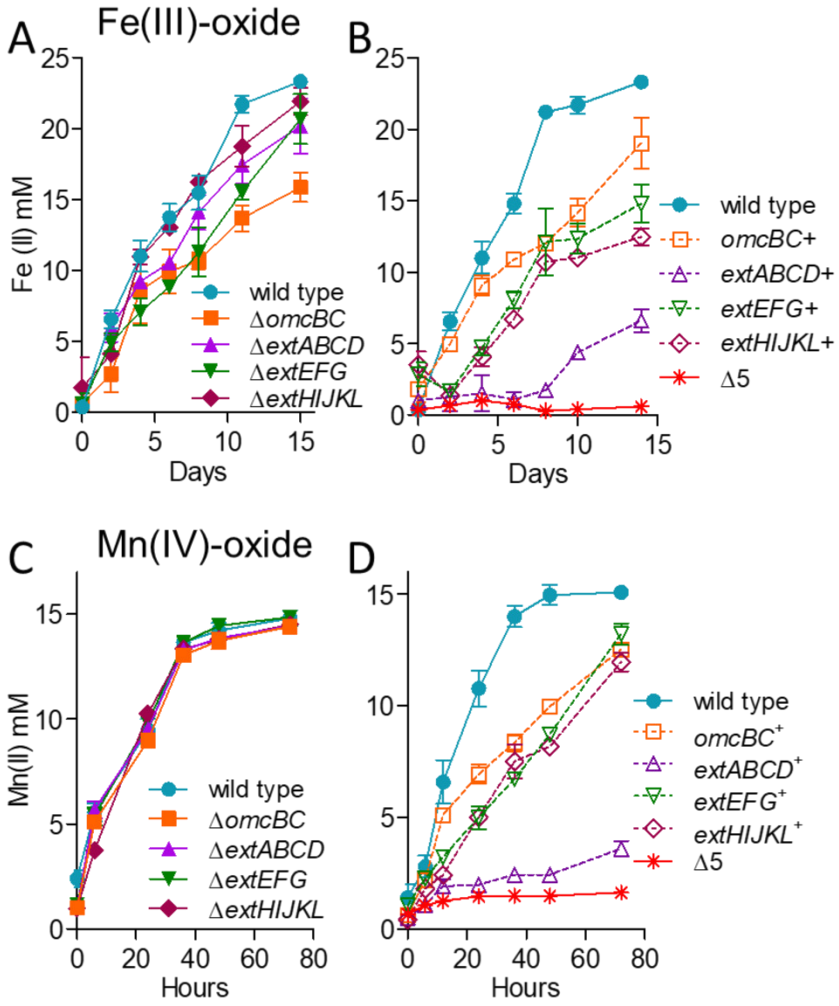

Figure 3. No single outer membrane cluster is essential but all are necessary for wild type levels of electron transfer to Fe(III)- and Mn(IV)-oxides. Growth of single cluster deletion mutants and triple mutants lacking all but one cytochrome conduit cluster, as well as the Δ5 mutant lacking all clusters utilizing A) 70 mM Fe(III)-oxide or B) 20 mM Mn(IV)-oxide as terminal electron acceptor. All experiments were conducted in triplicate and curves are average ± SD of n ≥ 3 replicates.

Figure 4.

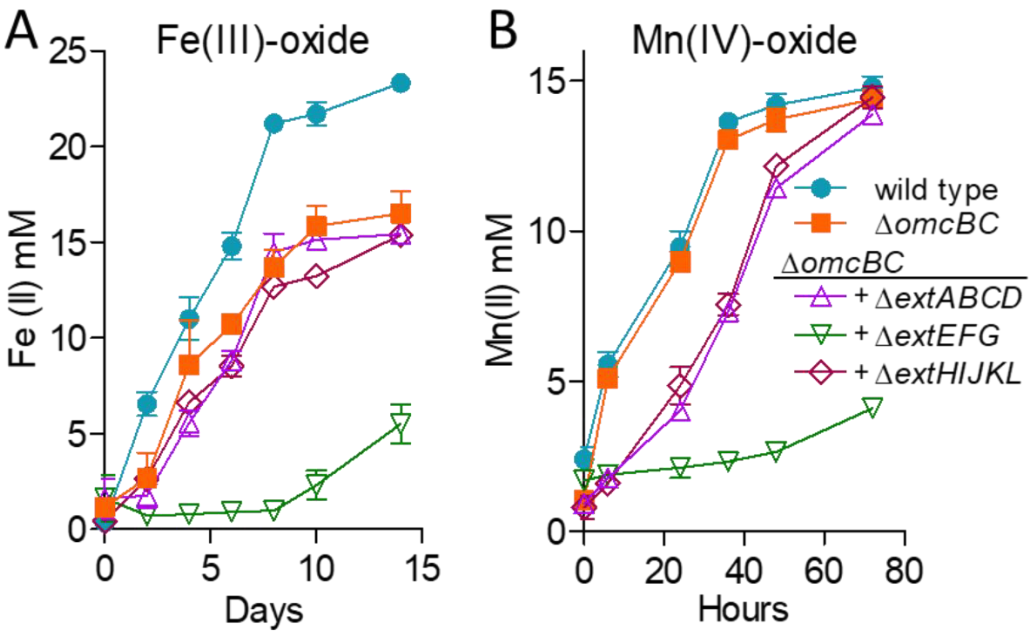

Figure 4. OmcBC and ExtEFG have additive roles in Fe(III)- and Mn(IV)-oxide reduction. Reduction of A) 70 mM Fe(III)-oxide or B) 20 mM Mn(IV)-oxide by the Δ*omcBC* strain and additional deletions in an Δ*omcBC* background. All experiments were conducted in triplicate and curves are average ± SD of n ≥ 3 replicates.

Figure 5.

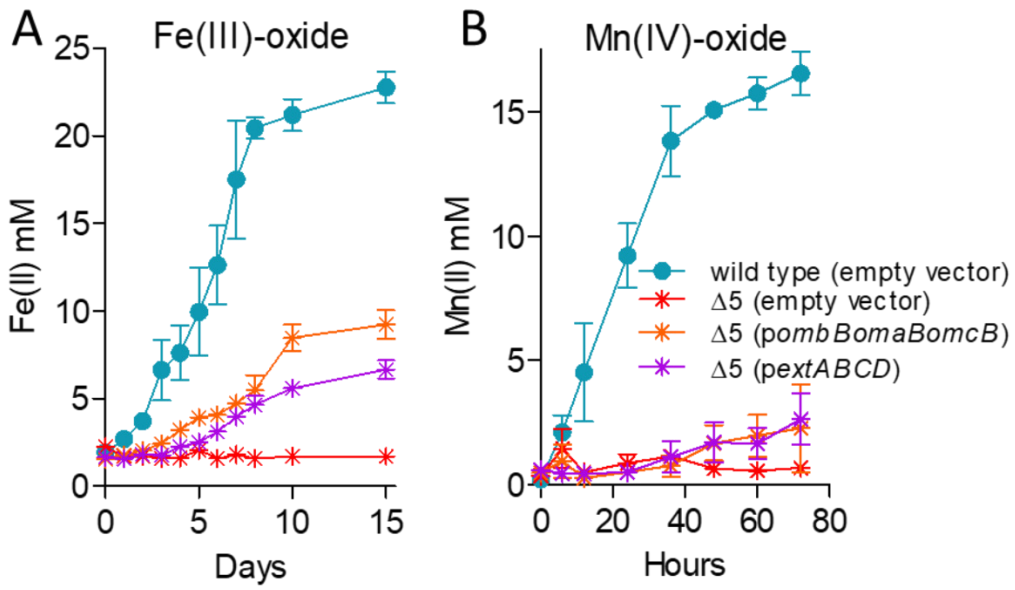

Figure 5. Partial complementation by single conduit clusters supports hypothesis that multiple conduit complexes are necessary for wild-type levels of metal oxide reduction. Reduction of A) 70 mM Fe(III)-oxide or B) 20 mM Mn(IV)-oxide by the Δ5 mutant expressing *extABCD* or the *omcB* cluster compared to the empty vector control. All experiments were conducted in triplicate and curves are average ± SD of n ≥ 3 replicates.

Figure 6

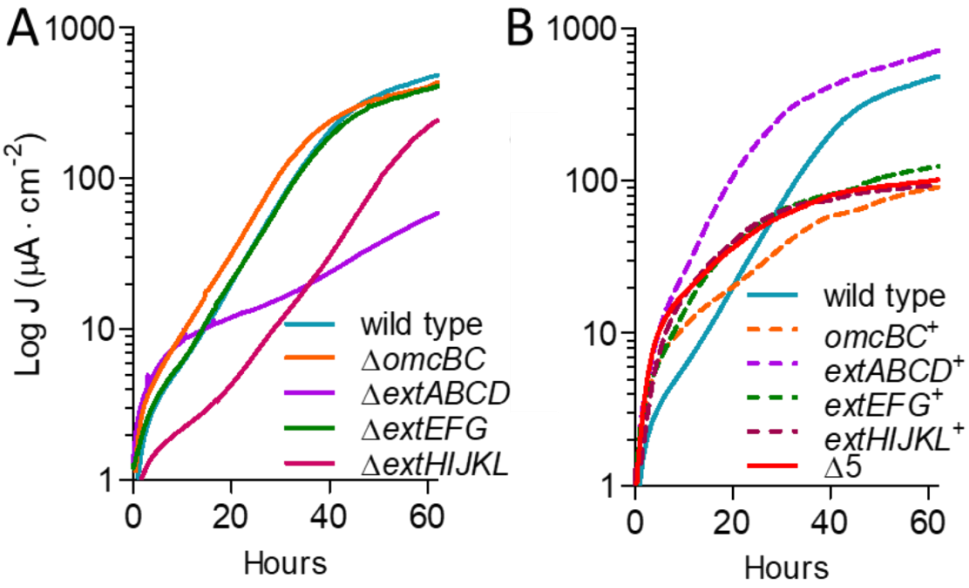

Figure 6. Only the ExtABCD conduit cluster is necessary for electrode reduction. Current density produced by A) single and B) multiple-cluster deletion mutants on graphite electrodes poised at +0.24 V vs. SHE. All mutants were grown in at least two separate experiments, and curves are representative of n ≥ 3 independent replicates per experiment. Similar results were obtained at lower (-0.1 V vs. SHE) redox potentials.

Figure 7.

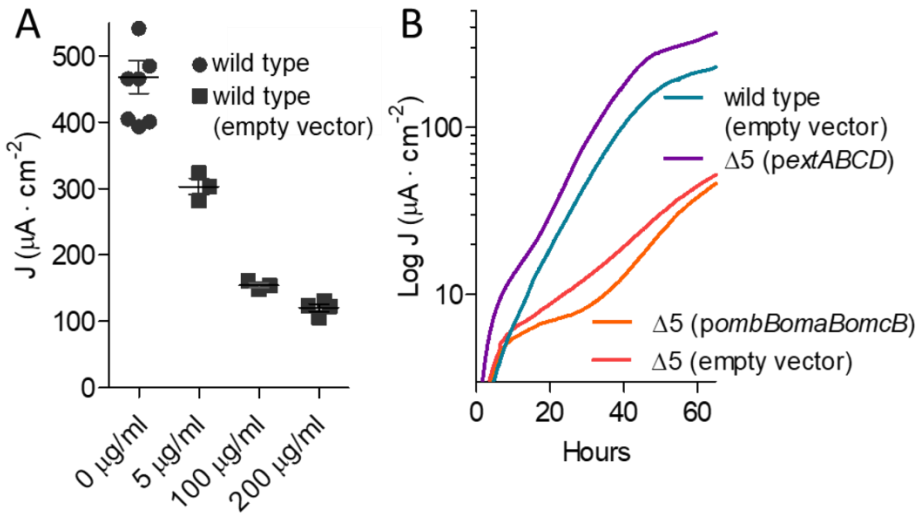

Figure 7. Effect of kanamycin on final current density, and comparison of ExtABCD and OmcBC complementation. A) Final current density of wild type *G. sulfurreducens* compared to wild type carrying an empty vector in the presence of increasing kanamycin concentrations. B) Current density produced by the Δ5 strain plus either *extABCD* or *omcB* cluster-containing vectors, in the presence of 5 μg/ml residual kanamycin. Wild type and Δ5 strains carrying the empty vector were used as controls. All experiments were conducted in duplicate and curves are representative of n ≥ 3 replicates per experiment.

Figure 8.

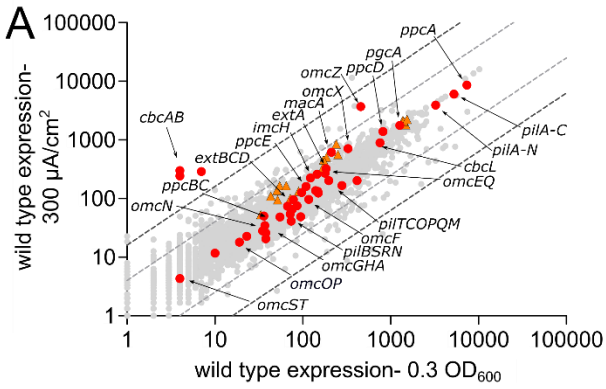

B

gene symbol	locus	annotation	RPKM fumarate	RPKM electrode	Log_2 change
cbcA	GSU0593	cytochrome b	4	301	6.23
cbcB	GSU0594	cytochrome c	4	242	5.92
omcZ	GSU2076	cytochrome c	456	3717	3.03
extD	GSU2642	lipoprotein cytochrome c	36	50	0.48
extC	GSU2643	lipoprotein cytochrome c	78	95	0.29
extB	GSU2644	OM integral protein	97	126	0.38
extA	GSU2645	cytochrome c	184	323	0.81
extG	GSU2724	cytochrome c	47	104	1.15
extF	GSU2725	lipoprotein cytochrome c	56	91	0.70
extE	GSU2726	OM integral protein	55	131	1.25
omcC	GSU2731	lipoprotein cytochrome c	261	803	1.62
omaC	GSU2732	cytochrome c	1455	1917	0.40
ombC	GSU2733	OM integral protein	1492	2038	0.45
omcB	GSU2737	lipoprotein cytochrome c	1614	1717	0.09
omaB	GSU2738	cytochrome c	1524	1971	0.37
ombB	GSU2739	OM integral protein	1667	2127	0.35
extL	GSU2936	hypothetical protein	59	157	1.42
extK	GSU2937	cytochrome c	70	158	1.18
extJ	GSU2938	hypothetical protein	272	534	0.97
extI	GSU2939	OM integral protein	201	480	1.26
extH	GSU2940	Iron-sulfur protein	187	434	1.21

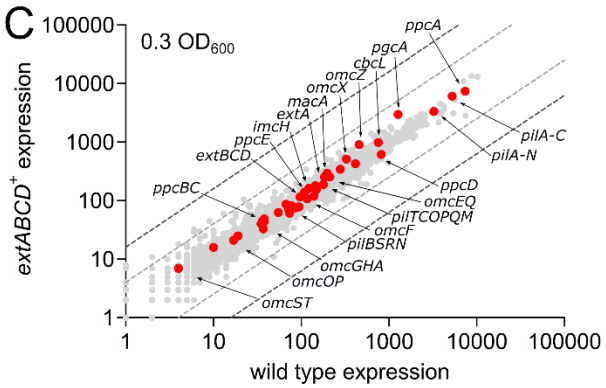

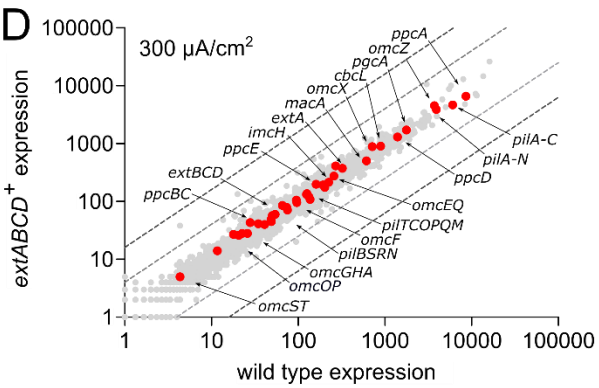

Figure 8. Transcriptomic analysis shows no significant differences in expression between *extABCD*$^+$ and wild type strains. . A) Comparison of expression levels of wild type exponentially growing cells under fumarate- and electrode-respiring conditions, showing no significant up- or downregulation of *ext* clusters.(orange triangles) or most other known electron transfer proteins (red circles). Dark and light gray dotted lines represent thresholds of 4 and 2 Log_2, respectively. B) RPKM and Log_2 change of ORFs with largest expression changes as well as genes studied in this work (for additional data, see Table S2). Comparison of the transcriptome of wild type and *extABCD*$^+$ cells exponentially growing using C) fumarate or D) electrode poised at +240 mV as terminal electron acceptor, showing no changes to electron transfer proteins due to deletion of *omBC, extEFG,* and *extHIJKL* clusters. Averages shown of biological replicate samples.

Figure 9.

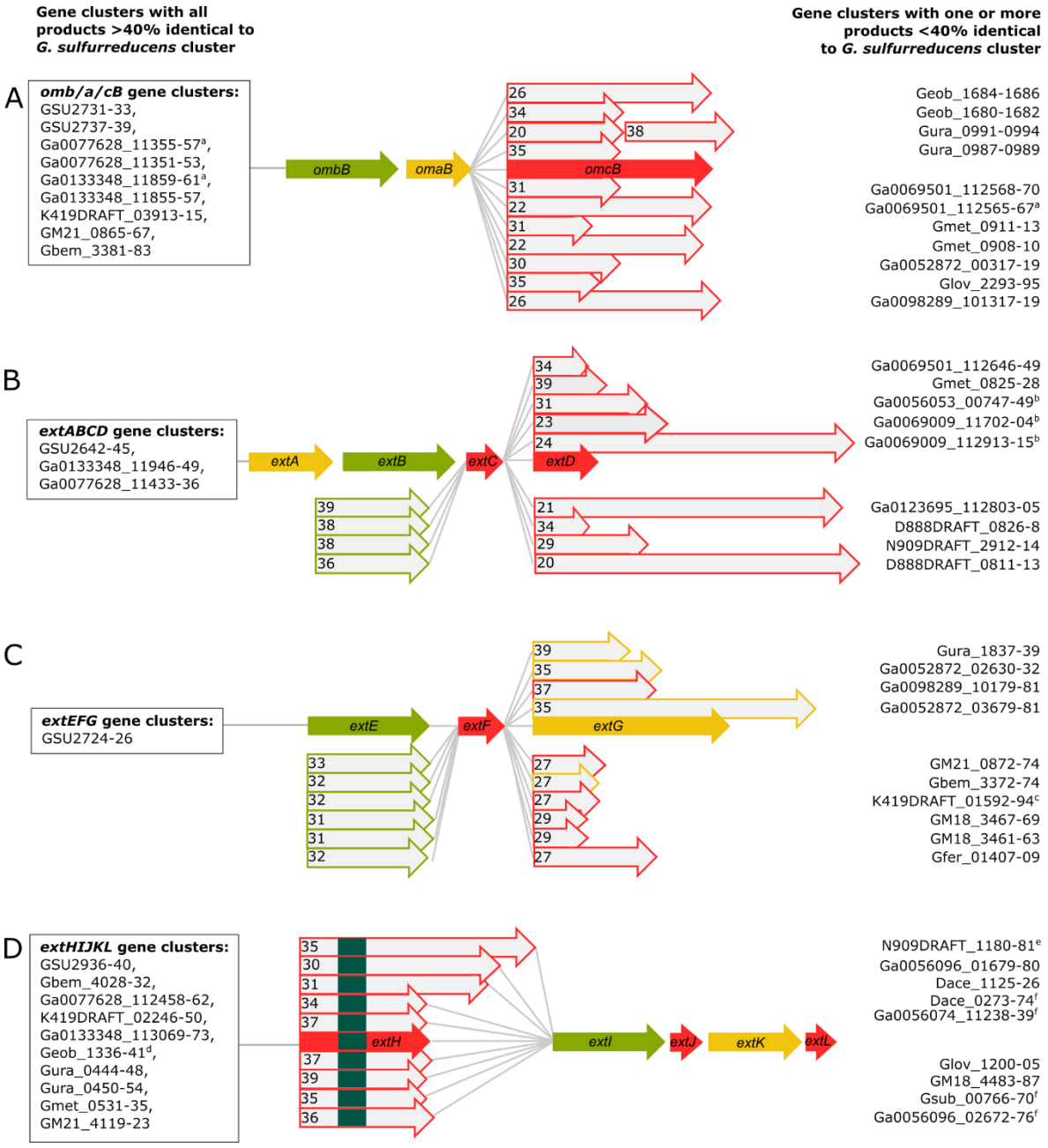

Figure 9. Cytochrome conduit conservation across the Order Desulfuromonodales. Representation of cytochrome conduit clusters from the Desulfuromonodales with homologs to either A) OmcBC, B) ExtABCD, C) ExtEFG, or D) ExtHIJKL. Red arrows = putative outer membrane products with a predicted lipid attachment site, yellow arrows = predicted periplasmic components, green arrows = predicted outer membrane anchor components. Complete clusters with all components sharing >40% identity to the corresponding *G. sulfurreducens* cytochrome conduit are indicated in boxes to the left of each gene cluster. Clusters in which one or more proteins are replaced by a new element with <40% identity are listed on the right

side of each gene cluster. Proteins with numbers indicate the % identity to the *G. sulfurreducens* version.

[a]OmcBC homologs in these gene clusters also encode Hox hydrogenase complexes. [b]Gene clusters have contiguous *extBCD* loci but *extA* is not in vicinity, as *extA* was found in separate parts of the genome for some of those organisms (see Supplemental Table S2). [c]Gene cluster has additional lipoprotein decaheme *c*-cytochrome upstream of *extE*. [d]Lipid attachment sites corresponding to ExtJL could not be found but there is an additional small lipoprotein encoded within the gene cluster. For ExtHIJKL clusters, homologs depicted above *extH* are found in gene clusters containing only *extI*, whereas homologs depicted below *extH* are found in gene clusters containing full *extHIJKL* loci. Upstream and on the opposite strand to all gene clusters homologous to *extHIJKL* there is a transcription regulator of the LysR family, except [e], where there is no transcriptional regulator in that region, and [f], where there are transcriptional regulators of the TetR family instead.